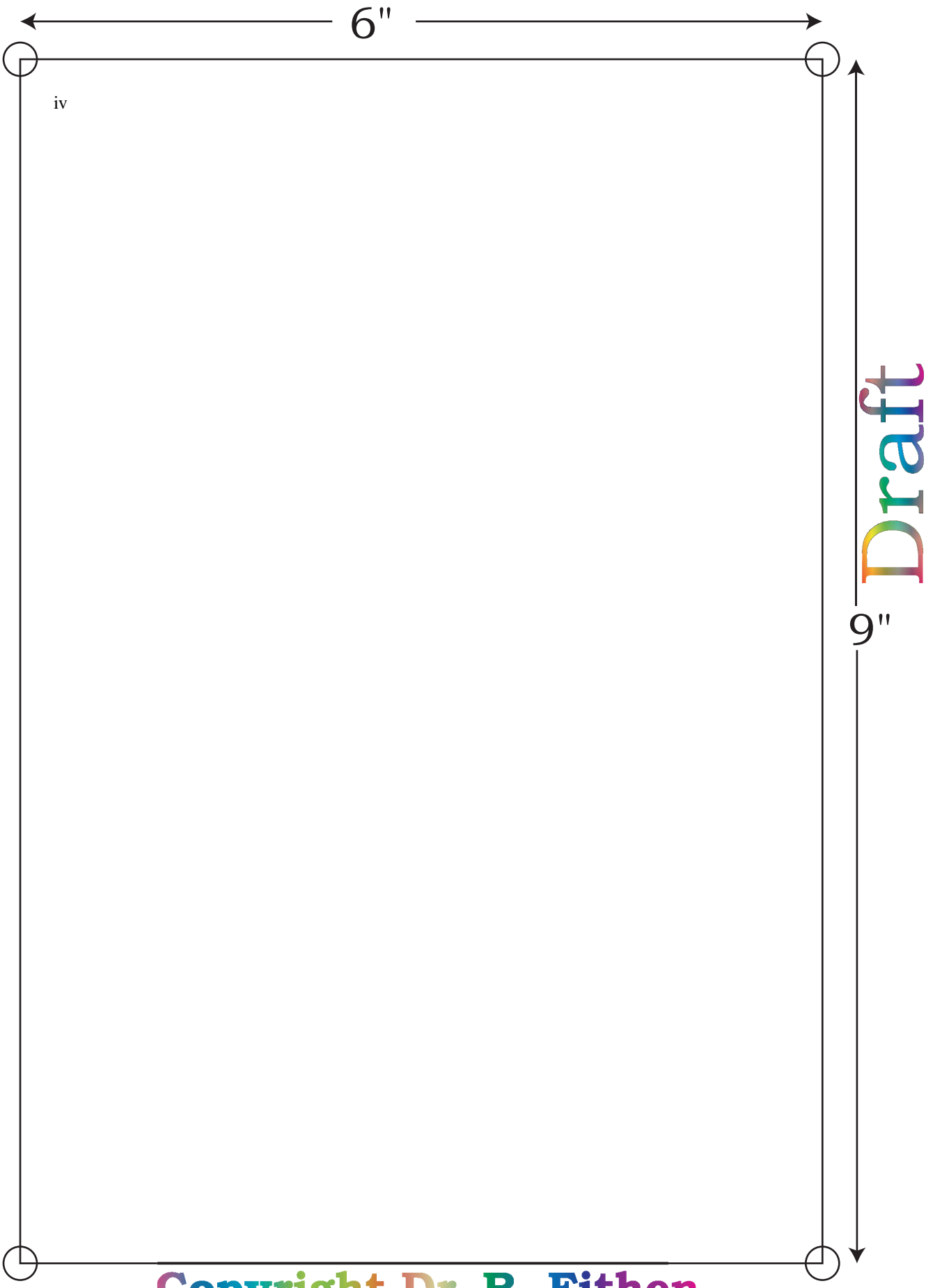
6"
9"
Draft

Finite Element Programming for Incompressible Fluids

© Dr. Robert M. Fithen

June 18, 2007

Copyright Dr. R. Fithen



Copyright Dr. R. Fithen

6"
9"
Draft

Contents

1 Fluid Flow Equations **1**
1.0.1 Convective Derivative . . . 3
1.1 Two Dimensional Unreduced Equations . . . 3
1.2 Two Dimensional Reduced Equations . . . 4
1.2.1 Stokes Flow . . . 5
1.3 Stokes Flow Solutions . . . 6
1.3.1 Poiseuille Flow . . . 6
1.3.2 Squeeze Plate . . . 8
1.3.3 Wannier Flow . . . 9
1.4 Navier-Stokes Solutions . . . 13
1.4.1 Kovasznay Flow . . . 13
1.4.2 Flow over a backstep . . . 13
1.4.3 Flow in a cavity . . . 14
1.4.4 Flow over a cylinder . . . 14

2 Finite Element Review **17**
2.1 Model Equation . . . 17
2.1.1 Weighted Residual Statement . . . 17
2.2 One-Dimensional Basis Functions . . . 19
2.2.1 Primal Basis Function . . . 19
2.2.2 Lagrange Elements . . . 20
2.2.3 Linear 1-D Lagrange Elements . . . 20
2.2.4 Quadratic 1-D Lagrange Elements . . . 21
2.2.5 Cubic 1-D Lagrange Elements . . . 22
2.2.6 Higher Order 1-D Spectral/Lagrange Basis Functions . . . 23
2.2.7 Hierarchial Basis Functions . . . 25
2.2.8 Legendre Polynomials . . . 25
2.2.9 Tchebychev Polynomials . . . 27
2.2.10 Orthogonal from Hierarchial Basis Functions . . . 28
2.3 Gram-Schmidt Orthonormalized Hierarchial Basis Functions . . . 32
2.4 Two Dimensional Basis Functions . . . 37
2.4.1 Primal Basis Function . . . 38
2.4.2 Primal to Linear Quadrilateral Mappings . . . 38
2.4.3 8-Noded Serendipity Element . . . 41
2.4.4 Two Dimensional Tensor Product Functions . . . 44

Copyright Dr. R. Fithen

2.4.5 Hierarchial Orthonormal Basis Functions (Mass Based) 46
2.4.6 Hierarchial Orthonormal Basis Functions (Stiffness Based) 52

3 Mixed Formulation **57**
3.0.7 Mixed Stokes equations 57

4 Penalty Formulation **61**

6"
9"
Draft
Copyright Dr. R. Fithen

6"
9"
Draft

Chapter 1

Fluid Flow Equations

In this chapter we present Navier-Stokes equations. Since it is assumed that the reader has had some type of fluid mechanics course, derivations of Navier-Stokes equations are referred to references [8, 16, 2, 10]. For those individuals familiar with indexed notation we will start with the complete Navier-Stokes/Continuity equations and reduce these equations down to incompressible, two dimensional equations. However, for those not familiar with index notation a convenient starting point begins with equation 1.19. These equations, 1.19 to 1.23, may be found in undergraduate fluids textbooks such as [8]. In indexed notation the continuity equation is:

$$\frac{\partial \rho}{\partial t} + \frac{\partial \rho u_k}{\partial x_k} = 0 \tag{1.1}$$

The Momentum equation in indexed notation can be written as:

$$\rho \frac{Du_j}{Dt} = \rho g_j + \frac{\partial \tau_{ij}}{\partial x_i} - \frac{\partial p}{\partial x_j} \tag{1.2}$$

Thermodynamic relations yield two equations:

$$\rho c_v \frac{DT}{Dt} + \rho T \left(\frac{\partial p}{\partial T}\right)_v \frac{Dv}{Dt} = -\frac{\partial q_k}{\partial x_k} + \tau_{ij} s_{ij} + G \tag{1.3}$$

$$\rho c_p \frac{DT}{Dt} - \rho T \left(\frac{\partial v}{\partial T}\right)_p \frac{Dp}{Dt} = -\frac{\partial q_k}{\partial x_k} + \tau_{ij} s_{ij} + G \tag{1.4}$$

The constitutive equations for both stress-velocity are:

$$\tau_{ij} = 2\mu s_{ij} \tag{1.5}$$

Where,

$$s_{ij} = \frac{1}{2}\left(\frac{\partial u_i}{\partial x_j} + \frac{\partial u_j}{\partial x_i}\right) - \frac{1}{3}\frac{\partial u_k}{\partial x_k}\delta_{ij} \tag{1.6}$$

Fourier's law of heat conduction is given by:

$$q_k = -\frac{\partial T}{\partial x_k} \tag{1.7}$$

Copyright Dr. R. Fithen

Throughout this text we consider *Only* Incompressible fluids. As a result the density (ρ) is constant with respect to time and space. Hence, the continuity equation becomes:

$$\cancelto{0}{\frac{\partial \rho}{\partial t}} + \rho \frac{\partial u_k}{\partial x_k} + u_k \cancelto{0}{\frac{\partial \rho}{\partial x_k}} = 0 \tag{1.8}$$

Where the terms with a downward arrow are equal to zero. As a result, the continuity equation becomes:

$$\frac{\partial u_k}{\partial x_k} = 0 \tag{1.9}$$

This equation may be used to reduce the momentum equations as well. We can immediately notice the constitutive equation 1.6 could be simplified to:

$$s_{ij} = \frac{1}{2}\left(\frac{\partial u_i}{\partial x_j} + \frac{\partial u_j}{\partial x_i}\right) - \frac{1}{3}\cancelto{0}{\frac{\partial u_k}{\partial x_k}}\delta_{ij} \tag{1.10}$$

However, before we use our continuity equation to simplify any form of the momentum equation we must be aware of a few facts. Use of the continuity equation in this manner will change the set of equations we will be *Numerically* solving. Although this change is subtle, it does change our boundary conditions, as we will see later. For now, we will not use the continuity equation to reduce the momentum equations.

Our two energy equations become the same equation for the case of incompressible fluids. Since the density, ρ, does not change as a function of space or time neither does the specific volume v. NOTE: $\rho = 1/v$. Therefore, the term Dv/Dt is zero. For a fixed pressure, the term $(\partial v/\partial T)_p$ is zero as well. In addition, the specific heats $c_v = c_p$ make each equation 1.3 and 1.4 exactly same, as shown in equation 1.11 below.

$$\rho c_v \frac{DT}{Dt} = -\frac{\partial q_k}{\partial x_k} + \tau_{ij} s_{ij} + G \tag{1.11}$$

In review, our set of equations for incompressible fluids are shown in equations 1.12 to 1.17.

Continuity:

$$\frac{\partial u_k}{\partial x_k} = 0 \tag{1.12}$$

Momentum:

$$\rho \frac{Du_j}{Dt} = \rho g_j + \frac{\partial \tau_{ij}}{\partial x_i} - \frac{\partial p}{\partial x_j} \tag{1.13}$$

Heat Transfer Equation:

$$\rho c_v \frac{DT}{Dt} = -\frac{\partial q_k}{\partial x_k} + \tau_{ij} s_{ij} + G \tag{1.14}$$

Constitutive Equations:

$$\tau_{ij} = \mu\left(\frac{\partial u_i}{\partial x_j} + \frac{\partial u_j}{\partial x_i}\right) \tag{1.15}$$

6" 9" Draft
Copyright Dr. R. Fithen

6"

$$s_{ij} = \frac{1}{2}\left(\frac{\partial u_i}{\partial x_j} + \frac{\partial u_j}{\partial x_i}\right) \tag{1.16}$$

$$q_k = -\frac{\partial T}{\partial x_k} \tag{1.17}$$

1.0.1 Convective Derivative

In the momentum and heat transfer equations, we have a convective derivative term on the left hand side of the equation. In each of these equations, the convective derivative can be written as in equation 1.18, see references [8], [16], [2] and [10] for a complete derivation and explanations.

$$\frac{DT}{Dt} = \frac{\partial T}{\partial t} + u_j \frac{\partial T}{\partial x_j} \tag{1.18}$$

From this point on the convective derivative will be written out in expanded from as shown in equation 1.18.

1.1 Two Dimensional Unreduced Equations

In this section, our indexed equations are written in standard cartesian form where u is the velocity in the x direction and v is the velocity in the y direction. The two dimensional form of Navier-Stokes equations, with heat ransfer, may be written as shown in equations 1.19 to 1.23. Notice there was no attempt to reduce the right hand side of the momentum equations using the new continuity equation, 1.9.

Continuity:

$$\frac{\partial u}{\partial x} + \frac{\partial v}{\partial y} = 0 \tag{1.19}$$

X-Momentum:

$$\rho\left(\frac{\partial u}{\partial t} + u\frac{\partial u}{\partial x} + v\frac{\partial u}{\partial y}\right) = \rho g_x + \frac{\partial}{\partial x}\underbrace{\left[2\mu\frac{\partial u}{\partial x}\right]}_{\tau_{xx}} + \frac{\partial}{\partial y}\underbrace{\left[\mu\left(\frac{\partial u}{\partial y} + \frac{\partial v}{\partial x}\right)\right]}_{\tau_{xy}} - \frac{\partial p}{\partial x} \tag{1.20}$$

Y-Momentum:

$$\rho\left(\frac{\partial v}{\partial t} + u\frac{\partial v}{\partial x} + v\frac{\partial v}{\partial y}\right) = \rho g_y + \frac{\partial}{\partial x}\underbrace{\left[\mu\left(\frac{\partial u}{\partial y} + \frac{\partial v}{\partial x}\right)\right]}_{\tau_{xy}} + \frac{\partial}{\partial y}\underbrace{\left[2\mu\frac{\partial v}{\partial y}\right]}_{\tau_{yy}} - \frac{\partial p}{\partial y} \tag{1.21}$$

Draft
9"
Copyright Dr. R. Fithen

Energy Equation:

$$\rho c_v \left(\frac{\partial T}{\partial t} + u\frac{\partial T}{\partial x} + v\frac{\partial T}{\partial y} \right) = \frac{\partial}{\partial x}\left(k\frac{\partial T}{\partial x} \right) + \frac{\partial}{\partial y}\left(k\frac{\partial T}{\partial y} \right) + \mu\Phi + G \tag{1.22}$$

Dissipation Function:

$$\Phi = 2\left[\left(\frac{\partial u}{\partial x} \right)^2 + \left(\frac{\partial v}{\partial y} \right)^2 \right] + \left(\frac{\partial u}{\partial y} + \frac{\partial v}{\partial x} \right)^2 \tag{1.23}$$

1.2 Two Dimensional Reduced Equations

In this section, the two dimensional form of the Navier-Stokes equations is reduced by using the modified continuity equation in equation 1.9. Using this equation in the X momentum equation we may reduce a portion of the equation as shown in equation 1.24.

$$\frac{\partial}{\partial x}\left[2\mu\frac{\partial u}{\partial x} \right] + \frac{\partial}{\partial y}\left[\mu\left(\frac{\partial u}{\partial y} + \frac{\partial v}{\partial x} \right) \right] = \mu\frac{\partial^2 u}{\partial x^2} + \mu\frac{\partial^2 v}{\partial y^2} + \mu\frac{\partial}{\partial x}\underbrace{\left[\frac{\partial v}{\partial y} + \frac{\partial u}{\partial x} \right]}_{=0} \tag{1.24}$$

Likewise this may be done on the Y momentum equation to give a new reduced set of equations. These equations are shown in equations 1.25 to 1.29.

Continuity:

$$\frac{\partial u}{\partial x} + \frac{\partial v}{\partial y} = 0 \tag{1.25}$$

X-Momentum:

$$\rho\left(\frac{\partial u}{\partial t} + u\frac{\partial u}{\partial x} + v\frac{\partial u}{\partial y} \right) = \rho g_x + \mu\left(\frac{\partial^2 u}{\partial x^2} + \frac{\partial^2 u}{\partial y^2} \right) - \frac{\partial p}{\partial x} \tag{1.26}$$

Y-Momentum:

$$\rho\left(\frac{\partial v}{\partial t} + u\frac{\partial v}{\partial x} + v\frac{\partial v}{\partial y} \right) = \rho g_y + \mu\left(\frac{\partial^2 v}{\partial x^2} + \frac{\partial^2 v}{\partial y^2} \right) - \frac{\partial p}{\partial y} \tag{1.27}$$

Energy Equation:

$$\rho c_v \left(\frac{\partial T}{\partial t} + u\frac{\partial T}{\partial x} + v\frac{\partial T}{\partial y} \right) = k\left(\frac{\partial^2 T}{\partial x^2} + \frac{\partial^2 T}{\partial y^2} \right) + \mu\Phi + G \tag{1.28}$$

6" 9" Draft
Copyright Dr. R. Fithen

6"

Dissipation Function:

$$\Phi = 2\left[\left(\frac{\partial u}{\partial x}\right)^2 + \left(\frac{\partial v}{\partial y}\right)^2\right] + \left(\frac{\partial u}{\partial y} + \frac{\partial v}{\partial x}\right)^2 \tag{1.29}$$

As we will see later in this text, these two formulations give different system equations as well as boundary conditions. Each formulation has its strengths and weakness depending on the problem we wish to solve.

1.2.1 Stokes Flow

Special mention should be made regarding the differences between Navier-Stokes equations and Stokes equations. If the flow situation is such that the convection term is negligible, then Navier-Stokes equation will reduce to Stokes equations. The only difference between Navier-Stokes and Stokes equations can be seen in the acceleration term on the left side of Navier-Stokes equations.

$$\frac{\partial \mathcal{Z}}{\partial t} + \underbrace{u\frac{\partial \mathcal{Z}}{\partial x}}_{=0} + \underbrace{v\frac{\partial \mathcal{Z}}{\partial y}}_{=0} \tag{1.30}$$

The continuity based reduced Stokes equations are shown in equations 1.31 - 1.35. Likewise, the unreduced Stokes equation results from removal of the same acceleration terms.

Continuity:

$$\frac{\partial u}{\partial x} + \frac{\partial v}{\partial y} = 0 \tag{1.31}$$

X-Momentum:

$$\rho\frac{\partial u}{\partial t} = \rho g_x + \mu\left(\frac{\partial^2 u}{\partial x^2} + \frac{\partial^2 u}{\partial y^2}\right) - \frac{\partial p}{\partial x} \tag{1.32}$$

Y-Momentum:

$$\rho\frac{\partial v}{\partial t} = \rho g_y + \mu\left(\frac{\partial^2 v}{\partial x^2} + \frac{\partial^2 v}{\partial y^2}\right) - \frac{\partial p}{\partial y} \tag{1.33}$$

Energy Equation:

$$\rho c_v\frac{\partial T}{\partial t} = k\left(\frac{\partial^2 T}{\partial x^2} + \frac{\partial^2 T}{\partial y^2}\right) + \mu\Phi + G \tag{1.34}$$

Dissipation Function:

$$\Phi = 2\left[\left(\frac{\partial u}{\partial x}\right)^2 + \left(\frac{\partial v}{\partial y}\right)^2\right] + \left(\frac{\partial u}{\partial y} + \frac{\partial v}{\partial x}\right)^2 \tag{1.35}$$

Notice the momentum equations are now linear. As we will find out later this linearity will allow for exact solutions to a particular class of problems. In addition, simulation of Stokes equations are not necessarily iterative in nature.

Draft
9"
Copyright Dr. R. Fithen

6"

We will study Stokes flow solutions extensively. Stokes flow simulations have one problem in common with full Navier-Stokes simulations, the pressure-velocity relationship. Since, the derivative on the pressure is first order and the derivative on the velocity is second order it stands to reason their basis functions should also follow this constraint. Later in this text we will perform several numerical experiments on by using different basis functions for the pressure and velocity. These experiments will be the basis for future selections with respect to the Navier-Stokes equations.

In the next several sections, exact solutions will be presented for Stokes equations. The only exception to this statement occurs in the *Kovasznay flow* section. Kovasznay flow is an exact solution to the full non-linear Navier-Stokes equation. As a result, this exact solution will be used for validation for the full Navier-Stokes equations.

1.3 Stokes Flow Solutions

In this section, we focus on analytical solutions to Stokes equations. Fortunately, all the solutions presented in this section are exact solutions. This fact makes it easy to compare our numerical solutions directly with an exact solution. In addition, Stokes equations are linear. As a result, iteration or time stepping will not be required to obtain a solution to these problems. The only exception to the previous statment lay in the segregated/approximate factorization methods presented later in this text.

1.3.1 Poiseuille Flow

The simplest exact solution to Navier-Stokes is that of Poiseuille flow. This flow situation is shown in 1.1. In this figure flow is from left to right through two infinite plates (top and bottom). The flow is fully developed. As a result there is no variation in the velocity with respect to the x coordinate. With this in mind the continuity equation, 1.25 becomes,

$$\frac{\partial v}{\partial y} = 0 \tag{1.36}$$

In addition, the momentum equations assuming steady state flow may be altered to give,
X-Momentum

$$0 = \mu\left(\frac{\partial^2 u}{\partial y^2}\right) - \frac{\partial p}{\partial x} \tag{1.37}$$

Y-Momentum:

$$0 = \rho g_y - \frac{\partial p}{\partial y} \tag{1.38}$$

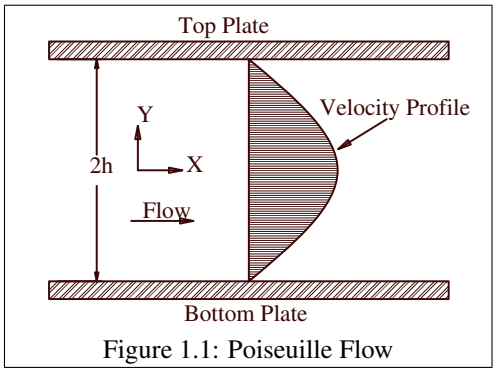


Figure 1.1: Poiseuille Flow

Assuming gravity only acts in the y direction we have a simple second order differential equation.

$$\mu\left(\frac{d^2 u}{dy^2}\right) = \frac{dp}{dx} \tag{1.39}$$

Draft
9"
Copyright Dr. R. Fithen

6"

Where $\frac{dp}{dx}$ is a prescribed constant value. Differentiating twice gives,

$$u = \frac{y^2}{2\mu}\left(\frac{dp}{dx}\right) + C_1 y + C_2 \tag{1.40}$$

Our origin is placed exactly half way between the infinite plates. In addition, the velocity is zero at $y = \pm h$. Hence, the equation for the velocity is:

$$\boxed{u = -\frac{h^2}{2\mu}\left(\frac{dp}{dx}\right)\left(1 - \frac{y^2}{h^2}\right)} \tag{1.41}$$

At this point we turn to Matlab in order to generate a plot of this solution. The Matlab code for this case is named `Poiseuille.m`. Executing this file under Matlab yields two plots as shown in figure 1.2.

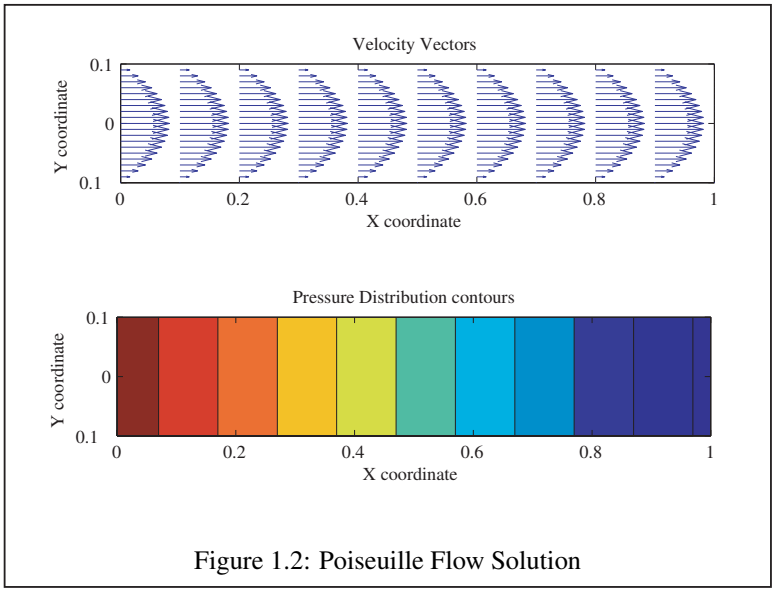


Figure 1.2: Poiseuille Flow Solution

Several interesting features to the exact solutions of Stokes(or Navier-Stokes) equations may be seen readily in this solution. If we look at our solution used in this example (and Matlab code `Poiseuille.m`) we may express these solutions as:

$$P = 45.34 - 2x \tag{1.42}$$

$$u = -0.01\left(1 - \frac{y^2}{0.01}\right) \tag{1.43}$$

One feature of this set of equations is that of the 45.34 in the pressure equation. Regardless of this value, the pressure gradient is still the same:

$$\frac{dP}{dx} = \frac{d}{dx}(45.34 - 2x) = -2 \tag{1.44}$$

Draft
9"
Copyright Dr. R. Fithen

6"

This means an arbitrary pressure may be added or subtracted from the pressure field with any change in the solution. This is *always* the case for incompressible flow fields (solutions). Another interesting observations may be made from these two equations. The velocity field is one order higher than the pressure field. In this case the velocity is second order (quadratic in y) in the independent variables. The pressure is first order (linear in x) in the independent variables. This will always be the case in incompressible flows. This fact can also be observed in equations 1.32 and 1.33, where a second order velocity derivative exists next to a first order pressure derivative. It would make sense that for these terms to exist in the same equation the velocity distribution must be one order higher than the pressure distribution. Both of these facts will play into how we develop numerical methods (finite element) for the solution of Navier-Stokes equations. As we will see later, there is some argument that the pressure should be approximated with one order lower element shape function than the velocities shape function. However, this requirement may be relaxed in certain formulations, while other formulations will require this shape function rule to be rigorously applied.

We shall use this exact solution later for validation purposes. However, such a simple solution will not push our numerical formulations. As a result we will seek out more complex exact solutions in the following sections for validations purposes.

1.3.2 Squeeze Plate

This flow situation is described by Nadai[9] and used by Reddy [13]. The flow condition may be seen in the figure below. In this case, the top and bottom plates are moving towards each

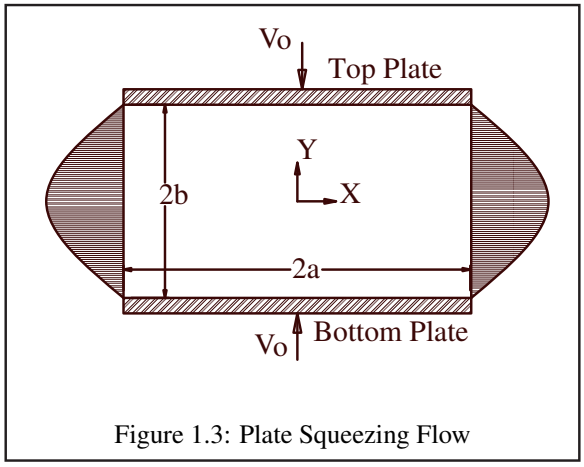


Figure 1.3: Plate Squeezing Flow

other with a velocity V_o. Consequently, the fluid is squeezed out both ends of the plates. The exact solution for this flow condition may be expressed as shown in the equations below:
Pressure

$$P = \frac{3\mu V_o}{2b^3}\left(a^2 + y^2 - x^2\right) \tag{1.45}$$

x-Velocity

$$u = \frac{3V_o x}{2b}\left(1 - \frac{y^2}{b^2}\right) \tag{1.46}$$

9"
Draft
Copyright Dr. R. Fithen

y-Velocity

$$v = -\frac{V_o y}{2b}\left(3 - \frac{y^2}{b^2}\right) \tag{1.47}$$

To test whether this solution satisfies the governing equations, we can used the symbolic portion of Matlab. To this end, the following Matlab code verifies that this set of equations 1.45, 1.45 and 1.45 do in fact satisfy the governing equations, 1.31, 1.32 and 1.33. The Matlab code that verified this is `PlateSqueezeExact.m`.

We now use Matlab to produce plots of this solution. Later in this text we shall use this section of code as a base line for validation of our finite element formulations. The Matlab code which will produce this plate squeezing case is `PlateSqueeze.m`. Using this Matlab file produces three plots as shown in figure 1.4. This flow situation is somewhat more

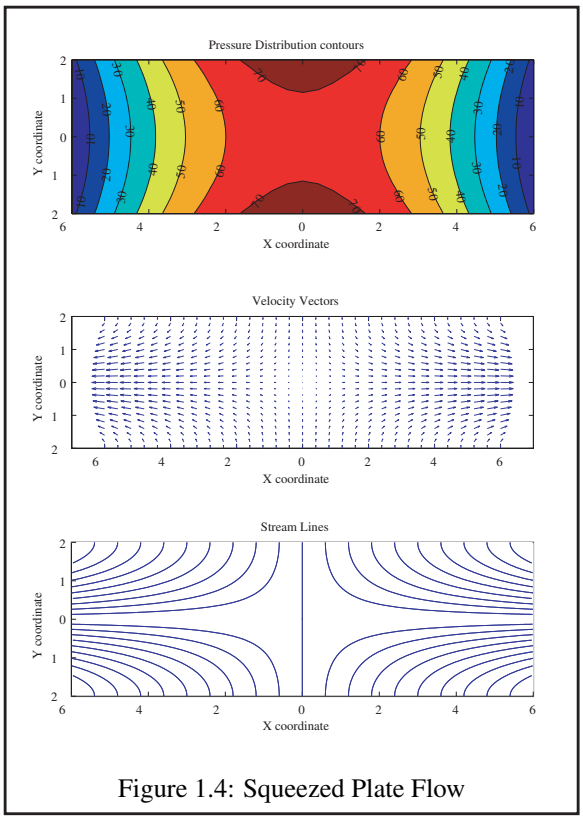


Figure 1.4: Squeezed Plate Flow

complicated than Poiseuille flow. As a result, it should offer a greater challenge to our finite element formulations. Again we may notice the form of the exact solution. The pressure is quadratic with respect to our spatial coordinates where the velocities are cubic.

1.3.3 Wannier Flow

Wannier flow [15] is one of the most complex Stokes solutions with regards to the domain's geometry and solution complexity. This analytic solution was developed with bearing lubrication in mind. As a result, the geometry consists of one cylinder offset inside another. From

6"
9"
Draft
Copyright Dr. R. Fithen

6"

Wannier's article, we have a geometry as shown in figure 1.5 In the previous analytical solu-

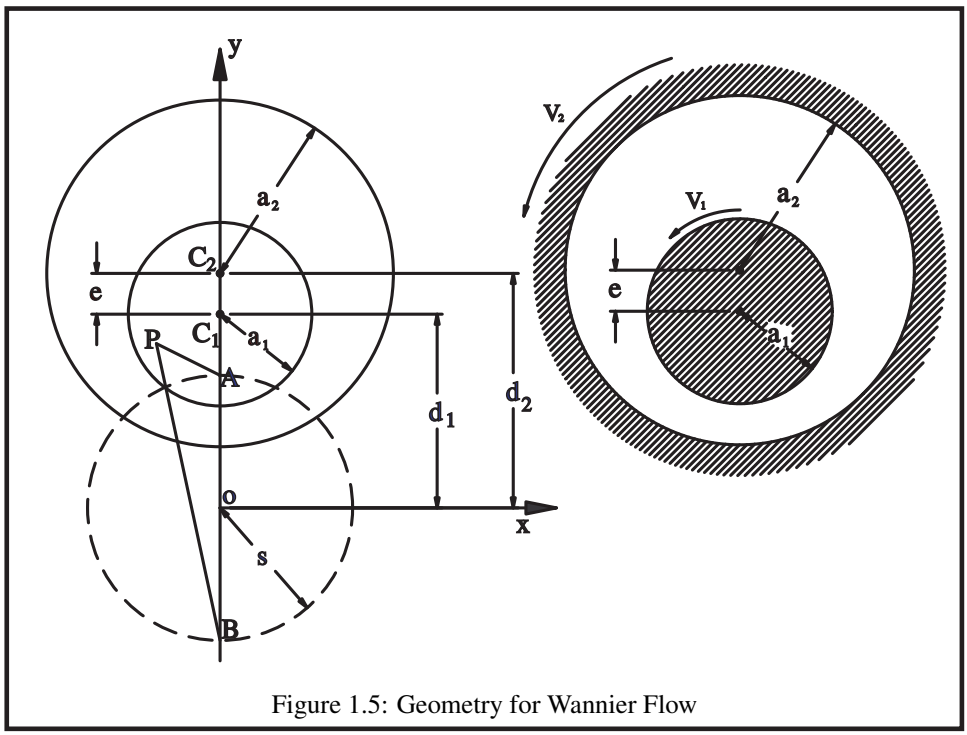


Figure 1.5: Geometry for Wannier Flow

tions, our problem geometry was a simple cartesian coordinate system. It is obvious from our figure that a much more complicated coordinate system will be required to work with Wannier flow. With this in mind, we turn to a coordinate system call *Bipolar Cylindrical*. Bipolar Cylindrical coordinate transformation may be written as,

$$x = \frac{a \sin \xi}{\cosh \eta - \cos \xi} \tag{1.48}$$

$$y = \frac{a \sinh \eta}{\cosh \eta - \cos \xi} \tag{1.49}$$

Since we will be working with this *orthogonal* coordinate system throughout our Wannier flow validations, it would seem prudent to go through the details of how this coordinate system will be used. Reproducing the drawing from Wannier's article as shown in figure 1.5, we can translate Wannier's information onto a Bipolar Coordinate system. From figure 1.5 we have,

$$d_1^2 - a_1^2 = d_2^2 - a_2^2 = s^2 \tag{1.50}$$

Given that,

$$d_2 - d_2 = e \tag{1.51}$$

We have the two relationships below:

$$d_1 = \frac{1}{2e}\left(a_2^2 - a_1^2\right) - \frac{1}{2}e \tag{1.52}$$

Draft
9"
Copyright Dr. R. Fithen

6"

$$d_2 = \frac{1}{2e}\left(a_2^2 - a_1^2\right) + \frac{1}{2}e \tag{1.53}$$

This geometry is used by Wannier to construct logarithmic potentials for the solution of Stokes equation. For our purposes, we need the variables d_1 and d_2 to construct our geometry through Bipolar Coordinates. A specific case of $a_1 = 0.5$, $a_2 = 4$ and $e = 2$ is shown in figure 1.6.

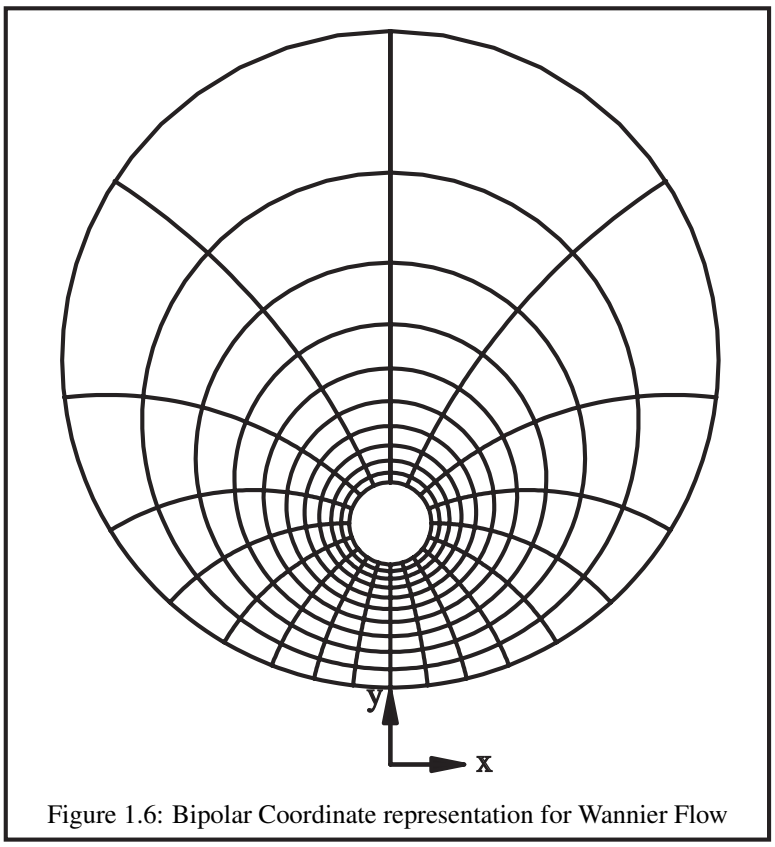


Figure 1.6: Bipolar Coordinate representation for Wannier Flow

It turns out that Bipolar coordinates line up perfectly with the construction of Wannier's solution. In addition, the fact that bipolar coordinates are orthogonal makes them especially attractive. Later we will use this bipolar coordinate system to map our elements onto this domain. The bipolar coordinate plot was created in Matlab using the code `BiPolarCoord.m`.

From Wannier's paper we have an exact solution to the streamfunction Ψ as shown in equation 1.54.

Draft
9"
Copyright Dr. R. Fithen

6"

$$\begin{aligned}\Psi =& A\ln\left[\frac{x^2+(s+y)^2}{x^2+(s-y)^2}\right]+B\ln\left[\frac{y\,(s+y)}{x^2+(s+y)^2}\right]\\&+C\left[\frac{y\,(s-y)}{x^2+(s-y)^2}\right]+Dy+E\left(x^2+y^2+s^2\right)\\&+Fy\ln\left[\frac{x^2+(s+y)^2}{x^2+(s-y)^2}\right]\end{aligned}\tag{1.54}$$

Where,

$$\mathcal{R}=\ln\left[\frac{(d_1+s)\,(d_2-s)}{(d_1-s)\,(d_2+s)}\right]\tag{1.55}$$

$$\mathcal{T}=\left(a_2^2+a_1^2\right)\mathcal{R}\tag{1.56}$$

$$\mathcal{Q}=\mathcal{T}-4se\tag{1.57}$$

$$\mathcal{Z}=\frac{2\left(d_2^2-d_1^2\right)\left(a_1v_1+a_2v_2\right)}{\left(a_2^2+a_1^2\right)\mathcal{Q}}+\frac{a_1^2a_2^2\left(a_1^{-1}v_1-a_2^{-1}v_2\right)}{s\left(a_1^2+a_2^2\right)\left(d_2-d_1\right)}\tag{1.58}$$

$$A=-\frac{1}{2}\left(d_2d_2-s^2\right)\mathcal{Z}\tag{1.59}$$

$$B=(d_1+s)\,(d_2+s)\,\mathcal{Z}\tag{1.60}$$

$$C=(d_1-s)\,(d_2-s)\,\mathcal{Z}\tag{1.61}$$

$$D=\frac{d_1\ln\left[\frac{d_2+s}{d_2-s}\right]-d_2\ln\left[\frac{d_1+s}{d_1-s}\right]}{\mathcal{Q}}\left(a_1v_1+a_2v_2\right)\tag{1.62}$$

$$E=\frac{\mathcal{R}}{2\mathcal{Q}}\left(a_1v_1+a_2v_2\right)\tag{1.63}$$

$$F=\frac{e}{2\mathcal{Q}}\left(a_1v_1+a_2v_2\right)\tag{1.64}$$

Using the bipolar coordinate system, we may plot an exact solution for any combination of a_1, a_2, e, v_1, and v_2. As an example, we select a case as shown in equation 1.65.

$$\boxed{\begin{aligned}a_1&=3\\a_2&=5\\e&=1.8\\v_1&=3\\v_2&=0\end{aligned}}\tag{1.65}$$

For these conditions, we use Bipolar Coordinates to lay out our solution in figures 1.7. The Matlab code that was used to produce this plot is `Wannier.m`. This routine constructs a mesh and places the solution on this mesh. The mesh is constructed using a bipolar coordinate system. The solution is then calculated and placed on this mesh for plotting.

This Matlab routine will be used extensively for validating our numerical schemes. Since Wannier flow is the most complex as far as geometry and solution complexity it will be considered the benchmark for Stokes flow throughout this text.

Draft
9"
Copyright Dr. R. Fithen

6"

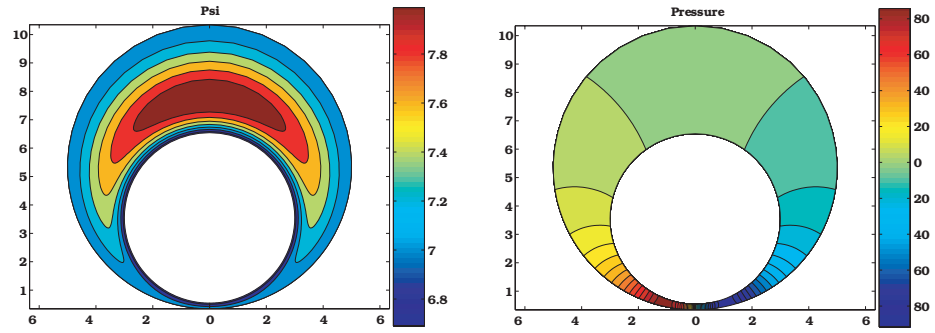


Figure 1.7: Pressure and ψ for Wannier Flow (Conditions above)

1.4 Navier-Stokes Solutions

In this section we focus on the solution to Navier-Stokes equations. Unlike the previous section we present only one exact solution to Navier-Stokes, Kovasznay Flow. All the other cases shown in this section are either taken from experiments or from previous numerical solutions.

1.4.1 Kovasznay Flow

Kovasznay [5] flow is a solution to full Navier-Stokes equation set 1.25-1.27. The flow situation is two-dimensional flow behind a grid. The exact solution is shown below.

$$u = 1 - e^{\lambda x}\cos(2\pi y) \tag{1.66}$$

$$v = \frac{\lambda}{2\pi}e^{\lambda x}\sin(2\pi y) \tag{1.67}$$

$$p = p_o - \frac{1}{2}e^{2\lambda x} \tag{1.68}$$

Where

$$\lambda = \frac{Re}{2} - \sqrt{\frac{Re^2}{4} + 4\pi^2} \tag{1.69}$$

There are several variables available to change the general behavior of our solution. First, the domain size may be changed. Also, the Reynolds number can be changed. For instructional purposes we chose a Reynolds number of 30 and a domain of $[-0.5, 2.5] \times [-1.0, 1.0]$.

The Matlab code `Kovasznay.m` was used to produced this plot. This code is very similar to previous codes that produced exact solutions on cartesian type grids.

1.4.2 Flow over a backstep

Flow over a backstep is one of the most common comparisons use to validate numerical schemes for full Navier-Stokes equations. The flow situation is shown in figure 1.9.

Since this solution is not exact it will not be a qualitative comparison. We shall compare our solution to that in reference [6] at several x locations down the backstep/channel.

9"
Draft
Copyright Dr. R. Fithen

6"

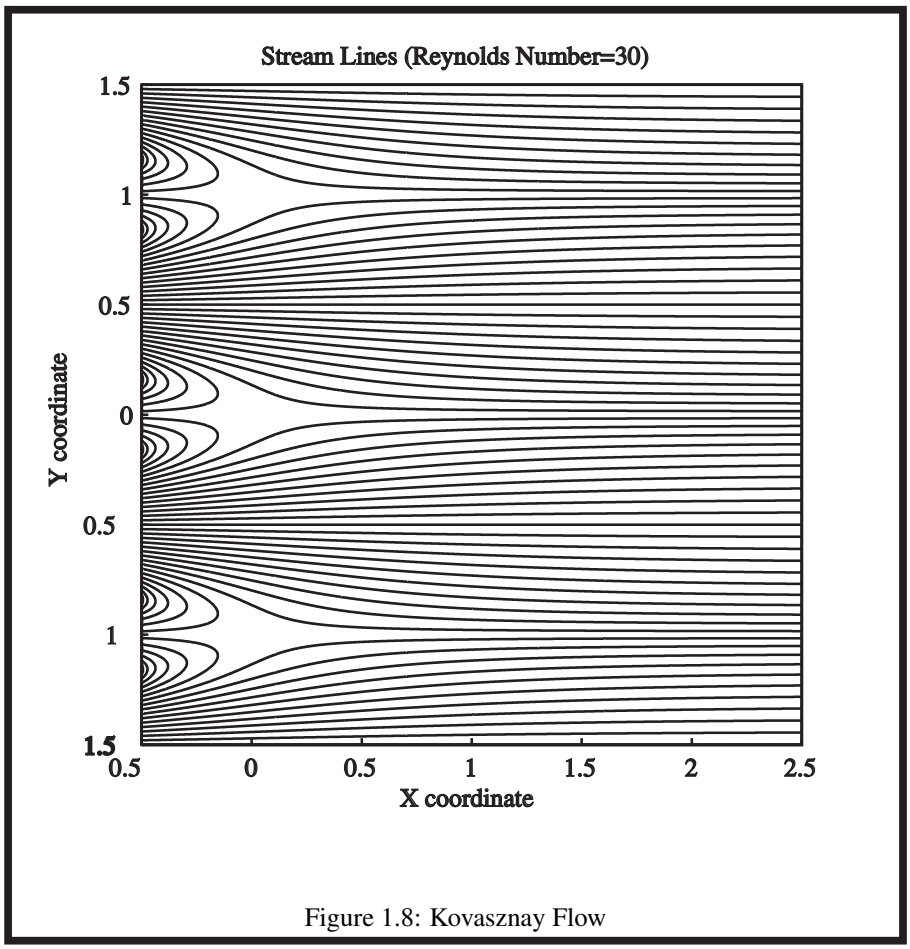


Figure 1.8: Kovasznay Flow

1.4.3 Flow in a cavity

Flow in a cavity is another of the most commonly used validation examples. Cavity flow has been used for decades as a validation case. As the computer speed have increased over time this problem is repeatedly presented with increased resolution. Interested reader are directed to [4] and all the references therein. The basic setup is on a unit square shown in figure 1.10

1.4.4 Flow over a cylinder

Flow over a cylinder is a benchmark problem for unsteady flows. At zero or low Reynolds number the flow field is steady in nature. However, as the Reynolds number rises the unsteady flow becomes a predominate factor.

9"
Draft
Copyright Dr. R. Fithen

6"

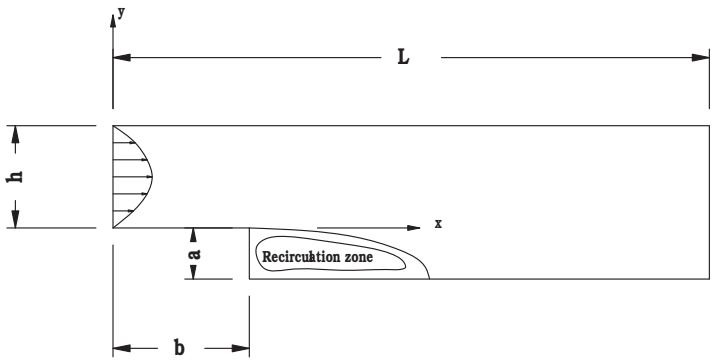


Figure 1.9: Backstep Geometry

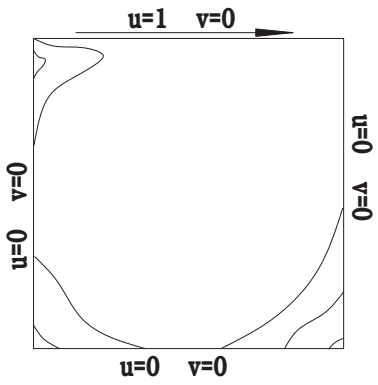


Figure 1.10: Cavity

Draft
9"
Copyright Dr. R. Fithen

6"
9"
Draft
Copyright Dr. R. Fithen

6"
9"
Draft

Chapter 2

Finite Element Review

In this chapter we review the basic finite element method. Since this text deals specifically with incompressible Navier-Stokes equations, only topics and methods in the finite element method dealing with this topic are covered. In addition, it is assumed the reader has some familiarity with the finite element method through and introductory text or course. With these assumptions we jump directly into two dimensional finite element method. As a model equations through this section we deal with a diffusion type equation.

2.1 Model Equation

As a model equation we begin with the anisotropic heat transfer equation 2.1.

$$-\overline{\nabla}\left(\overline{\overline{\mathcal{K}}}\,\overline{\nabla}T\right) = q \tag{2.1}$$

In this equation the conductivity term $\mathcal{K}$ is a full tensor as shown in equation 2.2.

$$\overline{\overline{\mathcal{K}}} = \begin{pmatrix} k_{11} & k_{12} & k_{13} \\ k_{21} & k_{22} & k_{23} \\ k_{31} & k_{32} & k_{33} \end{pmatrix} \tag{2.2}$$

If we focus, as we shall through most of this text, on two dimensional problems our model equation result in equation 2.3.

$$-\frac{\partial}{\partial x}\left(k_{11}\frac{\partial T}{\partial x} + k_{12}\frac{\partial T}{\partial y}\right) - \frac{\partial}{\partial y}\left(k_{21}\frac{\partial T}{\partial x} + k_{22}\frac{\partial T}{\partial y}\right) = q \tag{2.3}$$

2.1.1 Weighted Residual Statement

To obtain a weighted residual statement of our model equation we simple multiply by a weighting function and integrate this product over the entire domain of our problem of interest.

$$\int\int w_T\left[-\frac{\partial}{\partial x}\left(k_{11}\frac{\partial T}{\partial x} + k_{12}\frac{\partial T}{\partial y}\right) - \frac{\partial}{\partial y}\left(k_{21}\frac{\partial T}{\partial x} + k_{22}\frac{\partial T}{\partial y}\right) - q\right] dxdy = 0 \tag{2.4}$$

Copyright Dr. R. Fithen

6"

Integrating this equation by parts we obtain our finite element statement complete with our specification of our boundary conditions, 2.5

$$\begin{aligned}\int\int\left[\frac{\partial w_T}{\partial x}\left(k_{11}\frac{\partial T}{\partial x}+k_{12}\frac{\partial T}{\partial y}\right)+\frac{\partial w_T}{\partial y}\left(k_{21}\frac{\partial T}{\partial x}+k_{22}\frac{\partial T}{\partial y}\right)-w_T q\right]dxdy \\ -\oint w_T\left[\left(k_{11}\frac{\partial T}{\partial x}+k_{12}\frac{\partial T}{\partial y}\right)n_x+\left(k_{21}\frac{\partial T}{\partial x}+k_{22}\frac{\partial T}{\partial y}\right)n_y\right]dS=0\end{aligned} \tag{2.5}$$

If we designate our two boundary terms as shown in equations 2.6.

$$\begin{aligned}t_x&=\left(k_{11}\frac{\partial T}{\partial x}+k_{12}\frac{\partial T}{\partial y}\right)\\ t_x&=\left(k_{21}\frac{\partial T}{\partial x}+k_{22}\frac{\partial T}{\partial y}\right)\end{aligned} \tag{2.6}$$

our equations may be written as shown in equations 2.7.

$$\begin{aligned}\int\int\left[\frac{\partial w_T}{\partial x}\left(k_{11}\frac{\partial T}{\partial x}+k_{12}\frac{\partial T}{\partial y}\right)+\frac{\partial w_T}{\partial y}\left(k_{21}\frac{\partial T}{\partial x}+k_{22}\frac{\partial T}{\partial y}\right)\right]dxdy \\ =\int\int w_T q dxdy+\oint w_T\left(t_x n_x+t_y n_y\right)dS\end{aligned} \tag{2.7}$$

Using ψ as our finite element basis functions we have a system of equations as shown in equation 2.8.

$$\begin{aligned}\sum_{j=1}^{N}\left[\int\int\left[\frac{\partial\psi_i}{\partial x}\left(k_{11}\frac{\partial\psi_j}{\partial x}+k_{12}\frac{\partial\psi_j}{\partial y}\right)+\frac{\partial\psi_i}{\partial y}\left(k_{21}\frac{\partial\psi_j}{\partial x}+k_{22}\frac{\partial\psi_j}{\partial y}\right)\right]dxdy\right]T_j \\ =\int\int\psi_i q dxdy+\oint\psi_i\left(t_x n_x+t_y n_y\right)dS \qquad \forall \qquad i=1,2,3,\ldots,N\end{aligned} \tag{2.8}$$

If we adapt a matrix based symbolic approach as shown in equations 2.9 our equations become simplified as shown in equation 2.10. This simplification occurs only is our coefficients a_{11}, a_{12}, a_{21} and a_{22} are constants.

$$\begin{aligned}\mathcal{S}_{ij}^{xx}&=\int\int\frac{\partial\psi_i}{\partial x}\frac{\partial\psi_j}{\partial x}dxdy\\ \mathcal{S}_{ij}^{xy}&=\int\int\frac{\partial\psi_i}{\partial x}\frac{\partial\psi_j}{\partial y}dxdy\\ \mathcal{S}_{ij}^{yx}&=\int\int\frac{\partial\psi_i}{\partial y}\frac{\partial\psi_j}{\partial x}dxdy\\ \mathcal{S}_{ij}^{yy}&=\int\int\frac{\partial\psi_i}{\partial y}\frac{\partial\psi_j}{\partial y}dxdy\end{aligned} \tag{2.9}$$

$$\begin{aligned}\sum_{j=1}^{N}\left[k_{11}\mathcal{S}_{ij}^{xx}+k_{12}\mathcal{S}_{ij}^{xy}+k_{21}\mathcal{S}_{ij}^{yx}+k_{22}\mathcal{S}_{ij}^{yy}\right]T_j \\ =\int\int\psi_i q dxdy+\oint\psi_i\left(t_x n_x+t_y n_y\right)dS \qquad \forall \qquad i=1,2,3,\ldots,N\end{aligned} \tag{2.10}$$

Draft
9"
Copyright Dr. R. Fithen

If we write this system of equations in symbolic based matrix notation we we obtain equations 2.11 and 2.12.

$$\sum_{j=1}^{N} K_{ij} T_j = F_i \qquad \forall \qquad i = 1, 2, 3, \ldots, N \tag{2.11}$$

where

$$\begin{aligned} K_{ij} &= \left[k_{11}\mathcal{S}_{ij}^{xx} + k_{12}\mathcal{S}_{ij}^{xy} + k_{21}\mathcal{S}_{ij}^{yx} + k_{22}\mathcal{S}_{ij}^{yy} \right] \\ F_i &= \int\int \psi_i q dx dy + \oint \psi_i \left(t_x n_x + t_y n_y \right) dS \end{aligned} \tag{2.12}$$

These equations represent the finite element model of our model equation. In the next section we devote significant time and effort developing basis functions for use in this and other finite formulation.

2.2 One-Dimensional Basis Functions

In this section we devote our time and effort towards development of basis function for use in our finite element formulations. In this section we will deal with one dimensional basis functions. However, the goal in this section is setup to use these same one dimensional functions in our two dimensional basis functions. As we shall se later, this is accomplished through a tensor product type approach taking these very same one dimensional functions into higher dimensions.

2.2.1 Primal Basis Function

Primal basis functions are simply the basic polynomial terms used in any series. We may write a series solution to any problem as shown in equation 2.13

$$T(r) = \sum_{i=1}^{n} c_i \phi_i(r) \tag{2.13}$$

Where c_i are constants to be determined and $\phi_i(r)$ is our basis function set. In fact, the entire subject matter of the next several sections deals with selecting a basis function, $\phi_i(r)$'s, for our series. In this section we are looking for the simplest or a primal set of functions. With this in mind we consider a quadratic polynomial shown in equation 2.14

$$T(r) = c_1 + c_2 r + c_3 r^2 \tag{2.14}$$

From this equation we could easily see our simplest basis function set (primal basis functions) are the independent variables themselves, equation 2.15

$$\begin{aligned} \phi_1 &= 1 \\ \phi_2 &= r \\ \phi_3 &= r^2 \end{aligned} \tag{2.15}$$

6" 9" Draft
Copyright Dr. R. Fithen

These functions are never used directly in finite element practice. However, it is instructive to relate all basis functions back to this primal form to observe whether a given set of basis functions are complete. In fact, we will develop a transformation matrix from each our basis functions back to this primal basis set. This will also be used to observe the nature of each set of basis functions.

2.2.2 Lagrange Elements

One of the most common elements used today in the finite element community is called lagrange elements. The two dimensional form of these basis functions are tensor products of one dimensional lagrange elements. As a result, we shall look first at the one dimensional version of these basis functions.

It is common to write the one dimensional basis functions in a general form as shown in equation 2.16

$$\psi_i^r = \frac{\left[\prod_{j=1}^{j=(i-1)}(r-r_j)\right]\left[\prod_{j=(i+1)}^{j=n}(r-r_j)\right]}{\left[\prod_{j=1}^{j=(i-1)}(r_i-r_j)\right]\left[\prod_{j=(i+1)}^{j=n}(r_i-r_j)\right]} \tag{2.16}$$

2.2.3 Linear 1-D Lagrange Elements

As an example of a construction we begin with a one dimensional element as shown in figure 2.1 Since there are two nodes our basis functions from equation 2.16 are listed below in

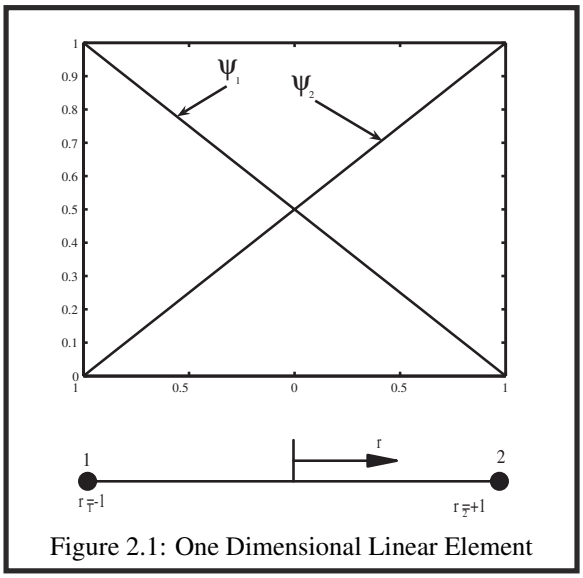


Figure 2.1: One Dimensional Linear Element

equation 2.17.

$$\begin{aligned}\psi_1^r &= \frac{(r-r_2)}{(r_1-r_2)} = \frac{(r-1)}{(-2)} = \frac{1}{2}(1-r)\\ \psi_2^r &= \frac{(r-r_1)}{(r_2-r_1)} = \frac{(r+1)}{(2)} = \frac{1}{2}(1+r)\end{aligned} \tag{2.17}$$

6"
9"
Draft
Copyright Dr. R. Fithen

Observing figure 2.1 we see the behavior of these elements. Each basis function is a value of unity at its designated node position and zero at all other nodal positions. These functions are of course linear in behavior between nodes.

2.2.4 Quadratic 1-D Lagrange Elements

Likewise, if we construct a quadratic one dimensional element as shown in 2.2 In this case,

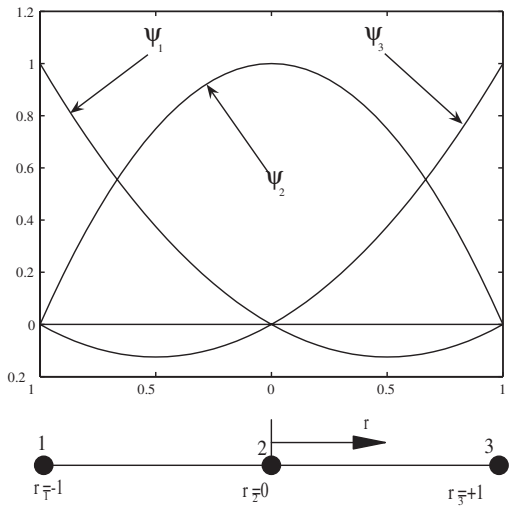


Figure 2.2: One Dimensional Quadratic Element.

there are three nodes our basis functions from equation 2.16 are listed below in equation 2.18.

$$\begin{aligned}\psi_1^r &= \frac{(r-r_2)(r-r_3)}{(r_1-r_2)(r_1-r_3)} \\ \psi_2^r &= \frac{(r-r_1)(r-r_3)}{(r_2-r_1)(r_2-r_3)} \\ \psi_3^r &= \frac{(r-r_1)(r-r_2)}{(r_3-r_1)(r_3-r_2)}\end{aligned} \tag{2.18}$$

Substituting values for r_1, r_2 and r_3 from figure 2.2 into these equations we obtain equation below, 2.19.

$$\begin{aligned}\psi_1^r &= \frac{1}{2}r(r-1) \\ \psi_2^r &= (r+1)(1-r) \\ \psi_3^r &= \frac{1}{2}r(r+1)\end{aligned} \tag{2.19}$$

These basis functions are shown in figure 2.2. Again we may notice the standard finite element lagrange approach of forcing the basis function to unity at their designated node while forcing the function to zero at all other nodes.

6"
9"
Draft
Copyright Dr. R. Fithen

2.2.5 Cubic 1-D Lagrange Elements

Constructing a cubic one dimensional element as shown in 2.3 In this case, there are four

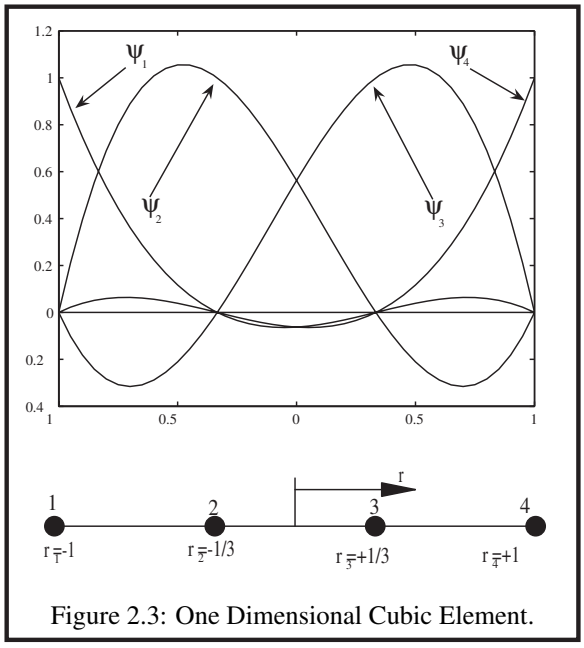


Figure 2.3: One Dimensional Cubic Element.

nodes our basis functions from equation 2.16 are listed below in equation 2.20.

$$\begin{aligned}
\psi_1^r &= \frac{(r-r_2)(r-r_3)(r-r_4)}{(r_1-r_2)(r_1-r_3)(r_1-r_4)} \\
\psi_2^r &= \frac{(r-r_1)(r-r_3)(r-r_4)}{(r_2-r_1)(r_2-r_3)(r_2-r_4)} \\
\psi_3^r &= \frac{(r-r_1)(r-r_2)(r-r_4)}{(r_3-r_1)(r_3-r_2)(r_3-r_4)} \\
\psi_4^r &= \frac{(r-r_1)(r-r_2)(r-r_3)}{(r_4-r_1)(r_4-r_2)(r_4-r_3)}
\end{aligned} \tag{2.20}$$

Substituting values for r_1, r_2, r_3 and r_4 from figure 2.3 into these equations we obtain equation below, 2.21.

$$\begin{aligned}
\psi_1^r &= \frac{\left(r+\frac{1}{3}\right)\left(r-\frac{1}{3}\right)(r-1)}{\left(-1+\frac{1}{3}\right)\left(-1-\frac{1}{3}\right)(-1-1)} = -\frac{9}{16}\left(r+\frac{1}{3}\right)\left(r-\frac{1}{3}\right)(r-1) \\
\psi_2^r &= \frac{(r+1)\left(r-\frac{1}{3}\right)(r-1)}{\left(-\frac{1}{3}+1\right)\left(-\frac{1}{3}-\frac{1}{3}\right)\left(-\frac{1}{3}-1\right)} = \frac{27}{16}(r+1)\left(r-\frac{1}{3}\right)(r-1) \\
\psi_3^r &= \frac{(r+1)\left(r+\frac{1}{3}\right)(r-1)}{\left(\frac{1}{3}+1\right)\left(\frac{1}{3}+\frac{1}{3}\right)\left(\frac{1}{3}-1\right)} = \frac{27}{16}(r+1)\left(r+\frac{1}{3}\right)(r-1) \\
\psi_4^r &= \frac{(r+1)\left(r+\frac{1}{3}\right)\left(r-\frac{1}{3}\right)}{(+1+1)\left(+1+\frac{1}{3}\right)\left(+1-\frac{1}{3}\right)} = -\frac{9}{16}(r+1)\left(r+\frac{1}{3}\right)\left(r-\frac{1}{3}\right)
\end{aligned} \tag{2.21}$$

6"
9"
Draft
Copyright Dr. R. Fithen

6"

These basis functions are shown in figure 2.3. The nodes are well defined in this plot where the functions are either zero or one. If we look at how these functions may be related as a function of the primal basis functions the use of a transformation matrix is shown below. In this equation we look at a 6^{th} order, 7 noded, Lagrange element. Notice the dependence on every basis function on the order. In essence every function is 6^{th} order as can be seen by observing the last column of the transformation matrix. We will see shortly how this is not the case for hierarchial basis functions.

$$\begin{pmatrix} \psi_1 \\ \psi_2 \\ \psi_3 \\ \psi_4 \\ \psi_5 \\ \psi_6 \\ \psi_7 \end{pmatrix} = \begin{bmatrix} 0 & -0.05 & 0.05 & 0.56 & -0.56 & -1.01 & 1.01 \\ 0 & 0.45 & -0.67 & -4.5 & 6.75 & 4.05 & -6.07 \\ 0 & -2.25 & 6.75 & 7.31 & -21.93 & -5.06 & 15.18 \\ 1 & 0 & -12.25 & 0 & 31.5 & 0 & -20.25 \\ 0 & 2.25 & 6.75 & -7.31 & -21.93 & 5.06 & 15.18 \\ 0 & -0.45 & -0.67 & 4.5 & 6.75 & -4.05 & -6.07 \\ 0 & 0.05 & 0.05 & -0.56 & -0.56 & 1.01 & 1.01 \end{bmatrix} \begin{pmatrix} 1 \\ r \\ r^2 \\ r^3 \\ r^4 \\ r^5 \\ r^6 \end{pmatrix} \tag{2.22}$$

2.2.6 Higher Order 1-D Spectral/Lagrange Basis Functions

In recent literature, see [3], the idea of spectral element methods have merged with the concepts of standard finite elements. At this point we take a simple concept from the spectral element community, nodal placement. It is common practice in the finite element community to place nodes equal distance across a higher order lagrange element. However, there is an advantage to distributing our nodes unequally across the element. We borrow this nodal placement concept from reference [3] as shown in equation 2.23.

$$r_j = \cos\left(\frac{\pi j}{N}\right) \tag{2.23}$$

In order to get a comparative between this nodal placement and standard equal-distant placement we look at a 7^{th} order element. Figure 2.4 shows a plot of the equal-distant nodal placement used in standard finite elements.

The nodal locations are easily observed on both plots. These nodal point are located where the basis functions are zero or one. In the spectral distribution the nodal points are clustered towards each end of the element. Another observation between the two functions is their overall maximums. The spectral nodal placement tends to result in a set of functions whose maximum is close to unity. By comparison the equal-distant nodal placement yields functions whose maximum are somewhat

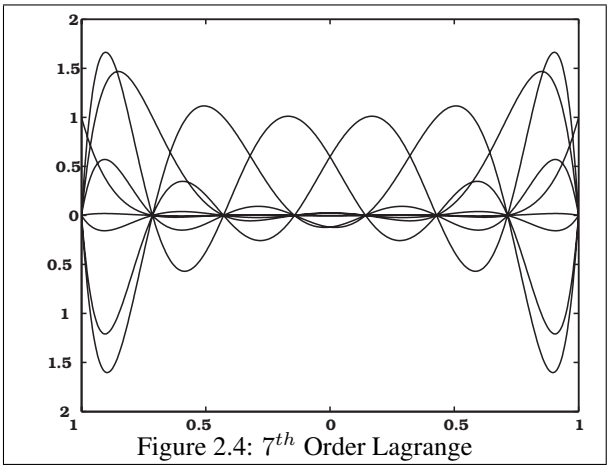


Figure 2.4: 7^{th} Order Lagrange

Draft
9"
Copyright Dr. R. Fithen

6"

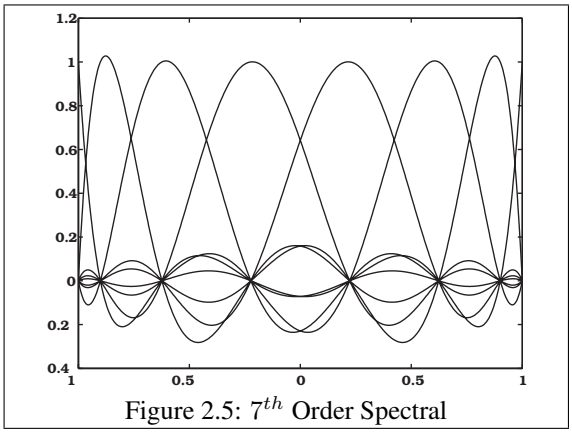


Figure 2.5: 7^{th} Order Spectral

higher. As an example, figure 2.6 shows a 17^{th} order basis function for both equal-distant and spectral nodal placements. The equal-distant nodal placement yields functional values around 300 where the spectral placement maximum is unity. It becomes quickly obvious that the equal-distant nodal placement results in extremely large functional values as the order of the basis functions are increased. However, this behavior is not observed in the spectral placement of nodes. Later we shall see more advantages to this spectral node placement. One final note should be made, for linear and quadratic basis functions the spectral and equal-distant nodal placement are exactly the same. The only difference between the nodal placement occurs from cubic order up.

Another advantage to spectral nodal placement occurs based on the numerical integration method used. Although we will make limited use of this placement through this text it is worth noting that the Chebyshev-Gauss-Lobatto integration rule is shown in equation 2.24.

$$x_i = \cos\left(\frac{\pi i}{N}\right) \qquad w_i = \begin{cases} \frac{\pi}{2N} & i = 0, N \\ \frac{\pi}{N} & 1 \leq i \leq N-1 \end{cases} \tag{2.24}$$

Using these integration points and a Chebyshev transformation we may develop an integration using Fast Fourier transforms. Interested reader may observe the discussion and accompanying computer codes in reference [3]. However, in this text will will do our best to avoid numerical integration due to the existence of Maple symbolic manipulation capability under Matlab. As a final note for this section all plots and conclusions may be obtained using the Matlab code named `LagrangeSpectral.m`.

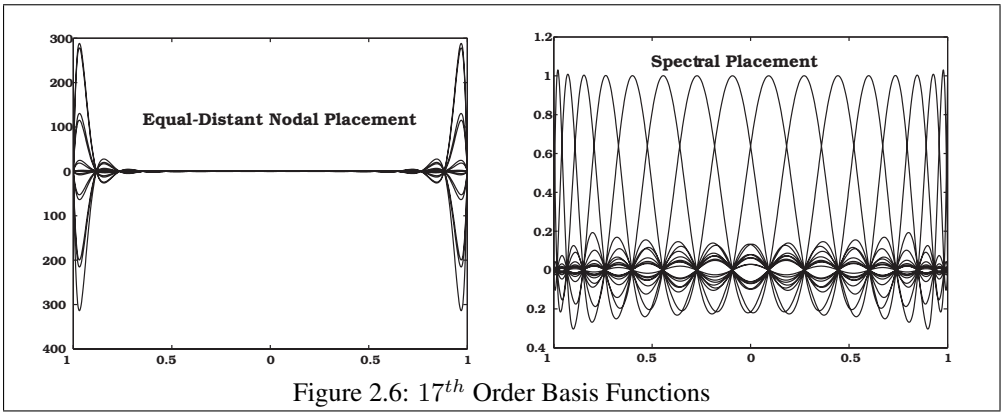


Figure 2.6: 17^{th} Order Basis Functions

Draft
9"
Copyright Dr. R. Fithen

6"

2.2.7 Hierarchial Basis Functions

Hierarchial basis functions gained popularity due to their ability to supply an adaptive solution capability. Their origins may be traced back to [11] and [12]. Detailed description may also be found in [14] and [17]. Hierarchial basis functions are constructed from a simple premise. All lower order basis functions exist explicitly in approximation. For example, in the Lagrange basis functions shown in figure 2.2 no functions from figure 2.1 exists. Compare this to a cubic hierarchial basis function as shown in figure 2.7. The unique feature of these basis functions is an embedding property. For example, a quadratic hierarchial basis function consist of basis functions, ψ_1, ψ_2 and ψ_3. While the cubic basis set consist of the quadratic basis set, ψ_1, ψ_2, ψ_3, in addition to the cubic function ψ_4. Since lower order basis function sets are always subsets of higher order, we only need to calculate the added functions when telescoping the series. These higher order enriching functions are the subject of ongoing research. There are several commonly accepted enriching functions in use today. However, since this is an area of ongoing research there are possible better enriching functions waiting to be discovered. We will cover a few of the common functions.

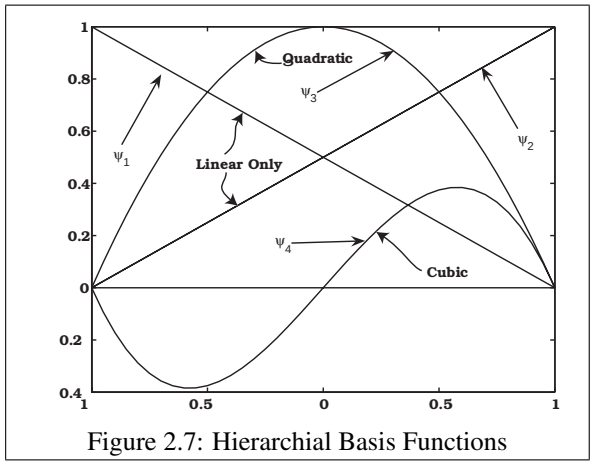


Figure 2.7: Hierarchial Basis Functions

2.2.8 Legendre Polynomials

Legendre polynomials originated from the solution of the Sturm-Liouville problem shown below in equation 2.25.

$$\frac{d}{dr}\left[\left(1-r^2\right)\frac{\mathcal{P}_k\left(r\right)}{dr}\right]+k\left(k+1\right)\mathcal{P}_k\left(r\right)=0 \tag{2.25}$$

in fact the Legendre polynomials are the eigenfunctions of this singular differential equation. The Legendre polynomial obey an interesting recurrence relationship shown in equations 2.26 to 2.28

$$\mathcal{P}_0\left(r\right)=1 \tag{2.26}$$

$$\mathcal{P}_1\left(r\right)=r \tag{2.27}$$

$$\mathcal{P}_{k+1}\left(r\right)=r\left[\frac{2k+1}{k+1}\right]\mathcal{P}_k\left(r\right)-\left[\frac{k}{k+1}\right]\mathcal{P}_{k-1}\left(r\right)\qquad\forall\, k\geq 2 \tag{2.28}$$

Another important property is the recursive derivative relationship shown in equation 2.29.

$$\frac{d\mathcal{P}_k\left(r\right)}{dr}=\frac{k\mathcal{P}_{k-1}\left(r\right)-kr\mathcal{P}_k\left(r\right)}{1-r^2} \tag{2.29}$$

Draft
9"
Copyright Dr. R. Fithen

Equations 2.25, 2.26 and 2.29 are proven in the Matlab file `SturmLiouvilleLegendre.m`. In this Matlab file, the recursion relationship, the differential relationship and the eigenfunction test are made. An abbreviated list of the Legendre functions are shown below in equation 2.30.

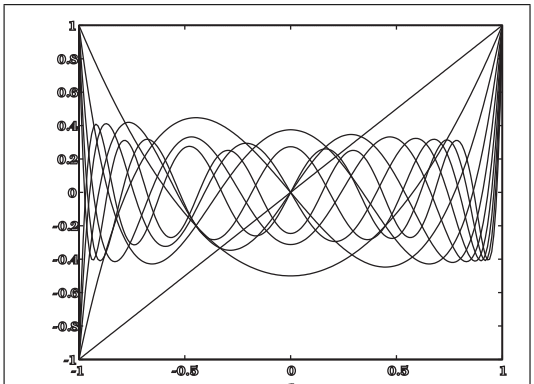


Figure 2.8: Legendre Polynomials

$$\begin{aligned}
\mathcal{P}_0(r) &= 1 \\
\mathcal{P}_1(r) &= r \\
\mathcal{P}_2(r) &= \frac{1}{2}\left(3r^2-1\right) \\
\mathcal{P}_3(r) &= \frac{1}{2}\left(5r^3-3r\right) \\
\mathcal{P}_4(r) &= \frac{1}{8}\left(35r^4-30r^2+3\right) \\
\mathcal{P}_5(r) &= \frac{1}{8}\left(63r^5-70r^3+15r\right)
\end{aligned} \tag{2.30}$$

How these functions are obtained is left to reference [1]. A plot of these functions are shown in figure 2.8. These functions may be split into odd and even numbered functions. In the Matlab code `legendre.m` this delineation is shown. All even numbered functions obey the end conditions $f(r=-1) = f(r=+1) = 1$. While all odd numbered functions obey the end conditions $f(r=-1) = -1$ and $f(r=+1) = 1$. In order to use these functions as hierarchial basis functions one requirement is all functions must be zero at the end points, $f(r=-1) = f(r=+1) = 0$. Noticing this pattern we could easily adjust our functions by using the first two Legendre polynomials to generate a new set of functions as shown in equation 2.31.

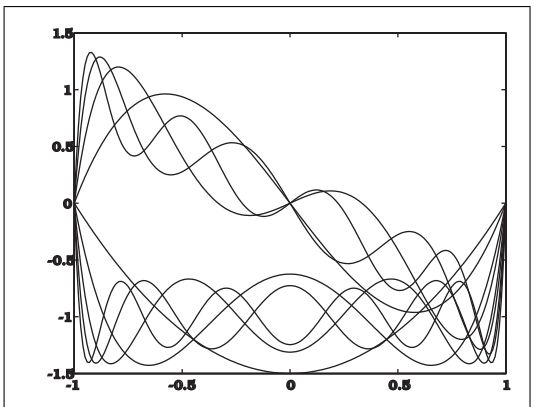


Figure 2.9: Legendre Basis Functions

$$\begin{aligned}
\psi_2(r) &= P_2(r) - P_0(r) \\
\psi_3(r) &= P_3(r) - P_1(r) \\
\psi_4(r) &= P_4(r) - P_0(r) \\
\psi_5(r) &= P_5(r) - P_1(r) \\
\psi_6(r) &= P_6(r) - P_0(r)
\end{aligned} \tag{2.31}$$

These functions are shown plotted in figure 2.9. In addition to the end requirements for hierarchial functions, they must also be complete. Legendre polynomials do satisfy this requirement and as a result are a reasonably good choice for our functions.

However, this is not the only choice for adjusting our Legendre polynomials. Another choice is shown in equations 2.32.

6" 9" Draft
Copyright Dr. R. Fithen

$$\begin{aligned}
\psi_2(r) &= P_2(r) - P_0(r) \\
\psi_3(r) &= P_3(r) - P_1(r) \\
\psi_4(r) &= P_4(r) - P_2(r) \\
\psi_5(r) &= P_5(r) - P_3(r) \\
\psi_6(r) &= P_6(r) - P_4(r)
\end{aligned} \tag{2.32}$$

This choice of functions result in a more palpable looking set when shown in a plot. This choice makes use of the fact that all even numbered functions have the same end conditions. Also all odd numbered functions have the same end conditions. As a result, we subtract the Legendre polynomial two orders back.

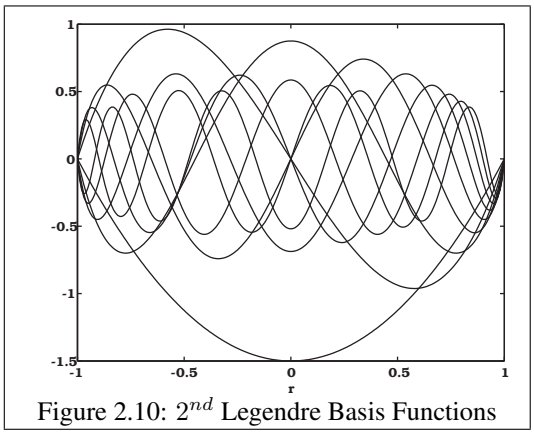


Figure 2.10: 2^{nd} Legendre Basis Functions

2.2.9 Tchebychev Polynomials

In this section we investigate the use of Tchebychev polynomials as basis functions. Tchebychev polynomials of the first kind come from the Sturm-Liouville differential equation of the form shown in equation 2.33.

$$\frac{d}{dr}\left[\sqrt{(1-r^2)}\frac{\mathcal{T}_k(r)}{dr}\right] + \frac{k^2}{\sqrt{(1-r^2)}}\mathcal{T}_k(r) = 0 \tag{2.33}$$

Just like Legendre polynomials, Tchebychev polynomials have a nice recurrence relationship. These recurrence relationship can be used in a subroutine to produce a polynomial of any order very quickly. The recursive relationship for Tchebychev polynomials are shown in equations 2.34 to 2.36.

$$\mathcal{T}_0(r) = 1 \tag{2.34}$$

$$\mathcal{T}_1(r) = r \tag{2.35}$$

$$\mathcal{T}_{k+1}(r) = 2r\mathcal{T}_k(r) - \mathcal{T}_{k-1}(r) \qquad \forall\ k \geq 2 \tag{2.36}$$

There are several relationships possible for the derivatives. However, we are interested in one which may be used in a subroutine. To this end we use equation 2.37

$$\frac{d\mathcal{T}_k(r)}{dr} = 2\mathcal{T}_{k-1}(r) + 2r\frac{d\mathcal{T}_{k-1}(r)}{dr} - \frac{d\mathcal{T}_{k-2}(r)}{dr} \qquad \forall\ k \geq 2 \tag{2.37}$$

An expanded set of these functions are listed in equation 2.38 below. 2.11

$$\begin{aligned}
\mathcal{T}_0(r) &= 1 \\
\mathcal{T}_1(r) &= r \\
\mathcal{T}_2(r) &= -1 + 2x^2 \\
\mathcal{T}_3(r) &= -3x + 4x^3 \\
\mathcal{T}_4(r) &= 1 - 8x^2 + 8x^4 \\
\mathcal{T}_5(r) &= 5x - 20x^3 + 16x^5
\end{aligned} \tag{2.38}$$

6"
9"
Draft
Copyright Dr. R. Fithen

6"

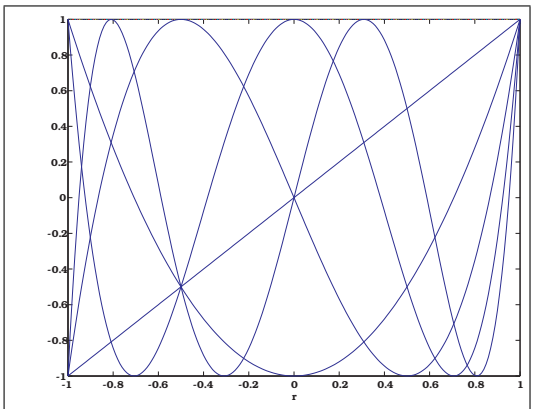


Figure 2.11: Tchebychev Polynomials

By comparing these functions with those in equation 2.30 we see the order of the functions are exactly the same, only the scale is different. A plot of these functions is shown in One particular thing to notice about Tchebychev polynomials is their magnitude. The maximum of all functional values is unity. This is due to the fact that Tchebychev polynomials are generated from a trigonometric transformation. Interested reader may consult reference [3] as well as the reference in their text.

Tchebychev polynomials suffer from the same fate as Legendre, that is their end conditions do not meet the requirement for hierarchial basis functions. Therefore, we take a similar approach, as in the Legendre function, to force our end conditions to zero. Namely the functions are altered as shown in equation 2.39

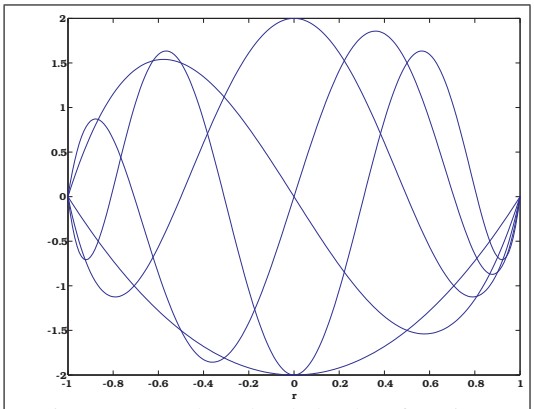


Figure 2.12: Altered Tchebychev functions

$$\begin{aligned}
\psi_2(r) &= T_2(r) - T_0(r) \\
\psi_3(r) &= T_3(r) - T_1(r) \\
\psi_4(r) &= T_4(r) - T_2(r) \\
\psi_5(r) &= T_5(r) - T_3(r) \\
\psi_6(r) &= T_6(r) - T_4(r)
\end{aligned} \tag{2.39}$$

A plot of these functions is shown in figure 2.12. Since we are subtracting two functions our new minimum and maximum is $|2|$ The distinction between Legendre and Tchebychev is very small. Both functions may be created through recursive relationships and both functions have a well defined derivative function. These two facts have help propel these two functions into the lime light as the hierarchial functions of choice.

2.2.10 Orthogonal from Hierarchial Basis Functions

Instead of covering numerous other possible hierarchial basis functions we will use our Legendre basis functions and adjust these functions to satisfy an interesting property. We will seek to satisfy some type of orthogonal condition, either through a mass type matrix of a stiffness matrix. We will begin this process using our one dimensional elements and extrapolate the process to two dimensional elements later.

One of the most common matrices that appear in finite element literature and methodology is that of a mass matrix. The Mass matrix is defined by equation 2.40 below.

$$M_{ij}^{\psi} = \int_{-1}^{+1} \psi_i(r)\,\psi_j(r)\,dr \tag{2.40}$$

Draft
9"
Copyright Dr. R. Fithen

6"

We begin with our basis functions as shown in equation 2.41.

$$\begin{aligned}
\psi_1 &= \frac{1}{2}(1-r) \\
\psi_2 &= \frac{1}{2}(1+r) \\
\psi_3 &= P_2(r) - P_0(r) \\
\psi_4 &= P_3(r) - P_1(r) \\
\psi_5 &= P_4(r) - P_2(r) \\
\psi_6 &= P_5(r) - P_3(r) \\
\psi_7 &= P_6(r) - P_4(r) \\
\psi_8 &= P_7(r) - P_5(r) \\
\psi_9 &= P_8(r) - P_6(r) \\
\psi_{10} &= P_9(r) - P_7(r)
\end{aligned} \tag{2.41}$$

Before we insert our basis functions into our we look back at equation 2.80 and observe the transformation matrix. In fact we can transform any basis function set into another through a similar transformation. We first look at the transformation between our new hierarchial basis functions and the primal basis functions. This transformation is shown in equation 2.42 below.

$$\begin{pmatrix} \psi_1 \\ \psi_2 \\ \psi_3 \\ \psi_4 \\ \psi_5 \\ \psi_6 \\ \psi_7 \end{pmatrix} = \frac{1}{16} \begin{bmatrix} 8 & -8 & 0 & 0 & 0 & 0 & 0 \\ 8 & 8 & 0 & 0 & 0 & 0 & 0 \\ -24 & 0 & 24 & \boxed{0} & \boxed{0} & \boxed{0} & \boxed{0} \\ 0 & -40 & 0 & 40 & \boxed{0} & \boxed{0} & \boxed{0} \\ 14 & 0 & -84 & 0 & 70 & \boxed{0} & \boxed{0} \\ 0 & 54 & 0 & -180 & 0 & 126 & \boxed{0} \\ -11 & 0 & 165 & 0 & -385 & 0 & 231 \end{bmatrix} \begin{pmatrix} 1 \\ r \\ r^2 \\ r^3 \\ r^4 \\ r^5 \\ r^6 \end{pmatrix} \tag{2.42}$$

Notice the zero terms in the boxes. By observation we see that our functions are in effect telescoping. In other words the third function is second order, the fourth function third order, the fifth function fourth order and so on. This fact is important because if one wish to increase the order of the approximation all lower order basis functions are exactly the same. Compare this transformation to that of the equal-distant Lagrange basis functions of the same order as shown in equation 2.22 and we see there is no telescoping possibility. In fact every entry in the transformation matrix is populated. Hence, every basis function in equation 2.22 is 6^{th} order. Comparing these two transformation one may readily see why the hierarchial basis functions have gain in popularity in the last several years.

We shall use our basis transformation concepts to develop a transformation between our hierarchial functions and a new set of functions. All basis transformations may be written as shown in equation 2.43.

$$\psi_i(r) = \mathcal{T}_{ik}^N \phi_k(r) \tag{2.43}$$

Where both ψ_i and ϕ_j are basis functions. The transformation matrix $\mathcal{T}_{ij}^N$ is similar to the matrix shown in equation 2.80. Using this transformation we may transform our mass matrix as shown in equation 2.44.

$$M_{ij}^{\psi} = \int_{-1}^{+1} \mathcal{T}_{ik}^N \phi_k(r) \mathcal{T}_{jl}^N \phi_l(r) \, dr = \mathcal{T}_{ik}^N \left[\int_{-1}^{+1} \phi_k(r) \phi_l(r) \, dr \right] \mathcal{T}_{jl}^N \tag{2.44}$$

Draft
9"
Copyright Dr. R. Fithen

Or

$$M_{ij}^{\psi} = \mathcal{T}_{ik}^{N} M_{kl}^{\phi} \mathcal{T}_{jl}^{N} \tag{2.45}$$

In standard matrix notation the matrix equation for this situation is shown below.

$$\left[M^{\psi}\right] = \left[\mathcal{T}^{N}\right] \left[M^{\phi}\right] \left[\mathcal{T}^{N}\right]^{T} \tag{2.46}$$

Looking closely at equation 2.46 and remembering information from eigenvalue/vector analysis, [7], this look very much like an eigenvalue/vector problem. If we attempt to approach this transformation as such the end result would be a diagonal matrix and completely altered basis functions. However, our approach will be that of altering only those hierarchial functions. As a result we must separate these basis functions through subdividing our matrices as shown in equation 2.47.

$$\begin{bmatrix} M_{11}^{\psi} & M_{12}^{\psi} \\ M_{21}^{\psi} & M_{22}^{\psi} \end{bmatrix} = \begin{bmatrix} \mathcal{T}_{11}^{N} & \mathcal{T}_{12}^{N} \\ \mathcal{T}_{21}^{N} & \mathcal{T}_{22}^{N} \end{bmatrix} \begin{bmatrix} M_{11}^{\phi} & M_{12}^{\phi} \\ M_{21}^{\phi} & M_{22}^{\phi} \end{bmatrix} \begin{bmatrix} \mathcal{T}_{11}^{N} & \mathcal{T}_{12}^{N} \\ \mathcal{T}_{21}^{N} & \mathcal{T}_{22}^{N} \end{bmatrix}^{T} \tag{2.47}$$

Where M_{11} are constructed from the first two non hierarchial basis functions. And, M_{22} is constructed from the hierarchial basis functions. Using this approach on we develop a new set of basis functions as shown in equation 2.48

$$\begin{pmatrix} \varphi_1 \\ \varphi_2 \\ \varphi_3 \\ \varphi_4 \\ \varphi_5 \\ \varphi_6 \\ \varphi_7 \end{pmatrix} = \begin{bmatrix} 1 & 0 & 0 & 0 & 0 & 0 & 0 \\ 0 & 1 & 0 & 0 & 0 & 0 & 0 \\ 0 & 0 & 0.103 & 0 & 0.562 & 0 & 0.821 \\ 0 & 0 & 0 & 0.420 & 0 & 0.907 & 0 \\ 0 & 0 & 0.187 & 0 & 0.800 & 0 & -0.571 \\ 0 & 0 & 0 & 0.907 & 0 & -0.420 & 0 \\ 0 & 0 & 0.977 & 0 & -0.212 & 0 & 0.022 \end{bmatrix} \begin{pmatrix} \psi_1 \\ \psi_2 \\ \psi_3 \\ \psi_4 \\ \psi_5 \\ \psi_6 \\ \psi_7 \end{pmatrix} \tag{2.48}$$

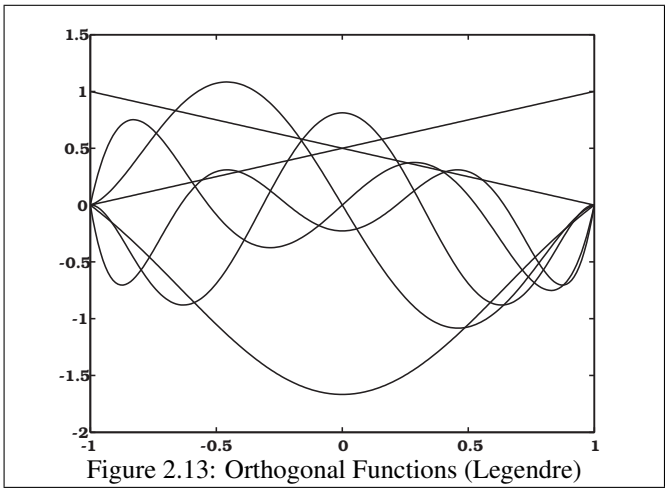


Figure 2.13: Orthogonal Functions (Legendre)

We may write this equations 2.51 and 2.42 in symbolic form as shown in equation 2.49.

$$\begin{aligned} \{\psi\} &= [Q]\{\phi\} \\ \{\varphi\} &= [T]\{\psi\} \end{aligned} \tag{2.49}$$

Where $\{\phi\}$ is the primal basis function set and $[Q]$ and $[T]$ are the transformation matrices in equations 2.51 and 2.42. From these equations we may obtain a transformation matrix from our new orthogonal basis functions to the primal basis functions. This new transformation matrix is obtained by simple substitution as shown in equation 2.50.

$$\{\varphi\} = [T][Q]\{\phi\} = [R]\{\phi\} \tag{2.50}$$

6"
9"
Draft
Copyright Dr. R. Fithen

It is instructive to observe this transformation for several reasons. The complete matrix is shown below in equation 2.51.

$$\begin{pmatrix} \varphi_1 \\ \varphi_2 \\ \varphi_3 \\ \varphi_4 \\ \varphi_5 \\ \varphi_6 \\ \varphi_7 \end{pmatrix} = \begin{bmatrix} 0.5 & -0.5 & 0 & 0 & 0 & 0 & 0 \\ 0.5 & 0.5 & 0 & 0 & 0 & 0 & 0 \\ -0.23 & 0 & 5.671 & 0 & -17.3 & 0 & 11.85 \\ 0 & 2.012 & 0 & -9.159 & 0 & 7.15 & 0 \\ 0.81 & 0 & -9.804 & 0 & 17.2 & 0 & -8.24 \\ 0 & -3.687 & 0 & 6.995 & 0 & -3.31 & 0 \\ -1.67 & -0 & 2.810 & 0 & -1.47 & 0 & 0.32 \end{bmatrix} \begin{pmatrix} \phi_1 \\ \phi_2 \\ \phi_3 \\ \phi_4 \\ \phi_5 \\ \phi_6 \\ \phi_7 \end{pmatrix} \tag{2.51}$$

We may quickly observe that our basis functions are no longer hierarchial. For example, φ_3 is a 6^{th} order function in r. Compare this to the general relation in hierarchial of φ_n is a $(n-1)^{th}$ order function in r. As a result it is not possible to increase the order of the approximation with destroying orthogonality. However, all is not lost. Later in this text we will use the method of hierarchial to orthogonal transformations, in conjunction with a substructuring to develop a systematic solution methodology for two dimensional analysis. A plot of these new orthogonal functions is shown in figure 2.13. These plots, as well as all conclusions, were generated from the Matlab file `LegendreMassMatrix.m`.

Interestingly enough, if we had used Tchebychev polynomials as the hierarchial basis functions the eignevalue/vector analysis would have yielded a different set of orthogonal functions. These functions are shown in figure 2.14. These plots, as well as all conclusions, were generated from the Matlab file `TchevMassMatrix.m`.

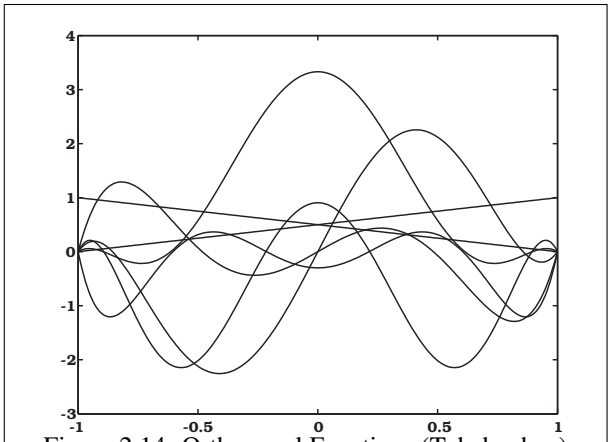


Figure 2.14: Orthogonal Functions (Tchebychev)

This brings up an interesting question: Is there some type of orthogonal basis functions that would be optimal? And what is the definition of the most optimal basis functions. One property that would definitely make our basis function selection optimal is that it is not only orthogonal, or better yet orthonormal, while still maintaining the property of hierarchial basis functions. The property to which we refer is, telescoping polynomial as shown through the transformation matrix 2.42. Better yet, it would be optimal if there were only one such set of functions for any given order to our polynomial. It would also be nice if this set of orthonormal-hierarchial basis functions could be generated from either Legendre or Tchebychev basis functions. Luckily, we can do all of the above by use of a Gram-Schmidt orthonormalization process. This is the focus of the next section.

6"
9"
Draft
Copyright Dr. R. Fithen

6"

2.3 Gram-Schmidt Orthonormalized Hierarchial Basis Functions

To accomplish the goals stated at the end of the last section we turn to the Gram-Schmidt process of orthonormalization. The process is well know and can be stated as follows.

Given a set of linearly independent functions $\{\phi_1, \phi_2, \phi_3, \phi_4, \ldots, \phi_n\}$. We may construct a an orthonormal set of functions $\{\psi_1, \psi_2, \psi_3, \psi_4, \ldots, \psi_n\}$ using the Gram-Schmidt process as defined below:

$$\psi_1 = \frac{\phi_1}{\sqrt{(\phi_1, \phi_1)}}$$

$$\widetilde{\psi}_2 = \phi_2 - (\psi_1, \phi_2)\,\psi_1$$

$$\psi_2 = \frac{\widetilde{\psi}_2}{\sqrt{\left(\widetilde{\psi}_2, \widetilde{\psi}_2\right)}}$$

$$\widetilde{\psi}_3 = \phi_3 - (\psi_1, \phi_3)\,\psi_1 - (\psi_2, \phi_3)\,\psi_2$$

$$\psi_3 = \frac{\widetilde{\psi}_3}{\sqrt{\left(\widetilde{\psi}_3, \widetilde{\psi}_3\right)}}$$

$$\widetilde{\psi}_4 = \phi_4 - (\psi_1, \phi_4)\,\psi_1 - (\psi_2, \phi_4)\,\psi_2 - (\psi_3, \phi_4)\,\psi_3$$

$$\psi_4 = \frac{\widetilde{\psi}_4}{\sqrt{\left(\widetilde{\psi}_4, \widetilde{\psi}_4\right)}}$$

$$\vdots$$

$$\widetilde{\psi}_n = \phi_n - (\psi_1, \phi_n)\,\psi_1 - (\psi_2, \phi_n)\,\psi_2 - (\psi_3, \phi_n)\,\psi_3 \cdots - (\psi_{n-1}, \phi_n)\,\psi_{n-1}$$

$$\psi_n = \frac{\widetilde{\psi}_n}{\sqrt{\left(\widetilde{\psi}_n, \widetilde{\psi}_n\right)}}$$

Mass Matrix Orthonormalization

In order to orthonormalize our mass matrix we must define our inner product, (ψ_i, ϕ_j), in such a way as to force this to occur. If we make out inner product as shown in equation 2.52 the mass matrix will be orthonormalize.

$$(\psi_i, \phi_j) = \int_{-1}^{+1} \psi_i(r)\,\phi_j(r)\,dr \tag{2.52}$$

One reason to focus on the orthonormalization of the mass matrix is its existence in time dependent problems. This is our reasoning for focusing on the mass ma-

Draft
9"
Copyright Dr. R. Fithen

6"

trix before the stiffness. If we take the Gram-Schmidt orthonormalization process to our Legendre and Tchebychev hierarchial basis functions we do in fact obtain the results we hoped for. Both basis functions yield the same exact orthonormal basis functions and the new functions are in fact hierarchial. In addition, adjusting either Legendre and Tchebychev functions through the Gram-Schmidt process can be done on the fly. This feature combined with the fact that the resulting basis functions are unique and telescoping mean these will be our functions of choice in both one and two dimensional problems. This fact makes these Gram-Schmidt based hierarchial functions telescoping. A plot of the new functions is shown in figure 2.15. The transformation between our new hierarchial orthonormal basis functions and the primal basis functions is shown in equation 2.53 below.

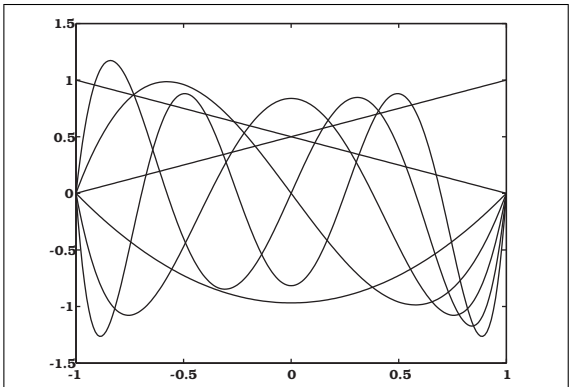


Figure 2.15: Orthonormal Basis Functions

$$\begin{pmatrix} \psi_1 \\ \psi_2 \\ \psi_3 \\ \psi_4 \\ \psi_5 \\ \psi_6 \\ \psi_7 \end{pmatrix} = \begin{bmatrix} 0.5 & -0. & 0 & 0 & 0 & 0 & 0 \\ 0.5 & 0. & 0 & 0 & 0 & 0 & 0 \\ -0.97 & 0 & 0.96 & \boxed{0} & \boxed{0} & \boxed{0} & \boxed{0} \\ 0 & -2.56 & 0 & 2.56 & \boxed{0} & \boxed{0} & \boxed{0} \\ 0.84 & 0 & -6.70 & 0 & 5.87 & \boxed{0} & \boxed{0} \\ 0 & 4.24 & 0 & -16.99 & 0 & 12.74 & \boxed{0} \\ -0.82 & 0 & 15.51 & 0 & -41.63 & 0 & 26.94 \end{bmatrix} \begin{pmatrix} 1 \\ r \\ r^2 \\ r^3 \\ r^4 \\ r^5 \\ r^6 \end{pmatrix} \tag{2.53}$$

Taking a look at the mass matrix is instructive at this point. Using these new orthonormal hierarchial basis function to generate a mass matrix results in equation 2.54

$$\begin{bmatrix} 0.667 & 0.333 & -0.645 & 0.342 & -0.224 & 0.162 & -0.124 \\ 0.333 & 0.667 & -0.645 & -0.342 & -0.224 & -0.162 & -0.124 \\ -0.645 & -0.645 & 1 & 0 & 0 & 0 & 0 \\ 0.342 & -0.342 & 0 & 1 & 0 & 0 & 0 \\ -0.224 & -0.224 & 0 & 0 & 1 & 0 & 0 \\ 0.162 & -0.162 & 0 & 0 & 0 & 1 & 0 \\ -0.124 & -0.124 & 0 & 0 & 0 & 0 & 1 \end{bmatrix} \tag{2.54}$$

One immediate property noticeable in this mass matrix is the appearance of an identity matrix embedded with the mass matrix. This in fact was our goal. By using Gram-Schmidt orthonormalization we have generated a mass matrix with this embedded identity matrix. This will occur regardless of the number of hierarchial basis functions we include. We shall use this embedded identity matrix later in the solution process by use of a substructuring type of solution approach. Interested reader should study the included Matlab file `GramSchmidtHierarchial.m` for complete details. This process will also be used later in two dimensional problems.

Draft
9"
Copyright Dr. R. Fithen

6"

Stiffness Matrix

To select a set of hierarchical basis functions that are orthonormal with respect to a stiffness matrix we must redefine our inner product term, (ψ_i, ϕ_j). To show that this process is the same for a stiffness matrix we take the example equation shown in equation 2.55 as our definition for (ψ_i, ϕ_j). Using the Gram-Schmidt process results in the same basis functions regardless of whether we start with Legendre or Tchebychev polynomials. Doing so we obtain the basis functions as shown in figure 2.16. Notice how this figure differs from that in figure 2.15. In fact, obtaining a basis function set which the hierarchial functions are orthonormal for the mass matrix and stiffness matrix is not possible unless we use the actual eigenfunctions for the given differential equation. As a result, we must choose which matrix we will force into a orthonormal state. This choice is related to not only the equation we wish to solve, but how we will be solving the equation. For example, if we wish to use a time dependent solution method to solve a steady state through time stepping the solution, forcing an orthonormal mass matrix is the best choice. Forcing an orthonormal stiffness matrix is best if we are solving a steady state problem in one step. Using the Matlab file `GramSchmidtHierarchialStiffness.m` we obtain the basis function set and the associate stiffness matrix, equation **??**.

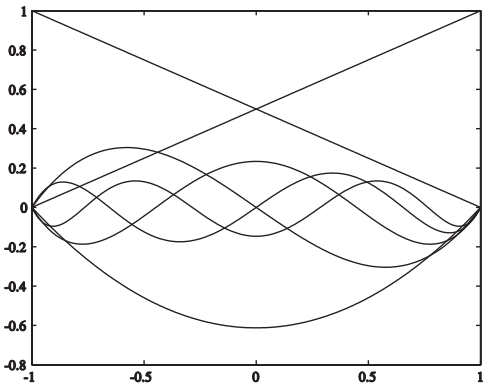


Figure 2.16: Orthonormal Basis Functions (Stiffness)

$$(\psi_i, \phi_j) = \int_{-1}^{+1} \frac{d\psi_i(r)}{dr} \frac{d\phi_j(r)}{dr} dr \tag{2.55}$$

Forcing the stiffness matrix into an orthonormal state results in the basis function shown below in equation 2.56. Notice the boxed zeros in boxes indicate this new basis function set is still hierarchial in nature.

$$\begin{pmatrix} \psi_1 \\ \psi_2 \\ \psi_3 \\ \psi_4 \\ \psi_5 \\ \psi_6 \\ \psi_7 \end{pmatrix} = \begin{bmatrix} 0.5 & -0.5 & 0 & 0 & 0 & 0 & 0 \\ 0.5 & 0.5 & 0 & 0 & 0 & 0 & 0 \\ -0.61 & 0 & 0.61 & \boxed{0} & \boxed{0} & \boxed{0} & \boxed{0} \\ 0 & -0.79 & 0 & 0.79 & \boxed{0} & \boxed{0} & \boxed{0} \\ 0.23 & 0 & -1.40 & 0 & 1.16 & \boxed{0} & \boxed{0} \\ 0 & 0.79 & 0 & -2.65 & 0 & 1.85 & \boxed{0} \\ -0.14 & 0 & 2.19 & 0 & -5.13 & 0 & 3.07 \end{bmatrix} \begin{pmatrix} 1 \\ r \\ r^2 \\ r^3 \\ r^4 \\ r^5 \\ r^6 \end{pmatrix} \tag{2.56}$$

Draft
9"
Copyright Dr. R. Fithen

6"

Notice the zeros in boxes indicate the basis function are hierarchial in nature. The stiffness matrix produced from this set of basis functions is shown in equation 2.57 below.

$$\begin{bmatrix} +0.5 & -0.5 & \boxed{0} & \boxed{0} & \boxed{0} & \boxed{0} & \boxed{0} \\ -0.5 & +0.5 & \boxed{0} & \boxed{0} & \boxed{0} & \boxed{0} & \boxed{0} \\ \boxed{0} & \boxed{0} & 1.0 & 0 & 0 & 0 & 0 \\ \boxed{0} & \boxed{0} & 0 & 1.0 & 0 & 0 & 0 \\ \boxed{0} & \boxed{0} & 0 & 0 & 1.0 & 0 & 0 \\ \boxed{0} & \boxed{0} & 0 & 0 & 0 & 1.0 & 0 \\ \boxed{0} & \boxed{0} & 0 & 0 & 0 & 0 & 1.0 \end{bmatrix} \tag{2.57}$$

At first glance it seems to be disturbing that the interactions between the linear basis functions and the hierarchial basis functions result in all zeros. As a result, zeros exist in the columns below and rows to the right of the original 2x2 linear basis functions, boxed zero terms. Therefore, the interaction between the original linear basis functions and the hierarchial basis functions are limited. To examine this situation further we take an example problem shown in equation 2.58 below.

$$\frac{d^2T}{dx} = \sin(3\pi x) \qquad 0 < x < 1 \tag{2.58}$$

For the given boundary conditions:

$$T(0) = T(1) = 0 \tag{2.59}$$

The exact solution to this differential equation is:

$$T(x) = -\frac{1}{9\pi^2}\sin(3\pi x) \tag{2.60}$$

We begin with a two element solution to this equation. To begin with we must resort to a element transformation often used in finite elements. The stiffness matrix must be altered through use of element mapping. This may occur by using the 2 mapping functions shown in the equation below.

$$\begin{aligned} x &= \frac{1}{4}(r_1 + 1) \\ x &= \frac{1}{4}(r_1 + 3) \end{aligned} \tag{2.61}$$

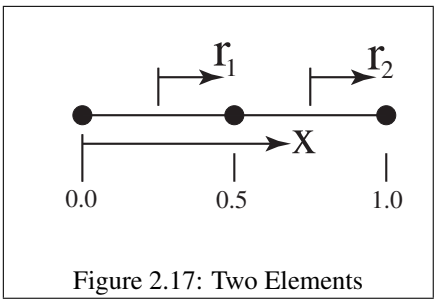


Figure 2.17: Two Elements

Which may be rearranged such that the local independent variable r may be expressed as a function of the global variable x.

$$\begin{aligned} r_1 &= 4x - 1 \\ r_2 &= 4x - 3 \end{aligned} \tag{2.62}$$

As a result of this mapping we have a differential relationship as,

$$\frac{dr_i}{dx} = 4 \tag{2.63}$$

Draft
9"
Copyright Dr. R. Fithen

6"

With this relationship in mind we look at our stiffness equation through the eyes of a mapping and obtain,

$$K_{ij} = \int_{x_l}^{x_r} \frac{d\psi_i}{dx}\frac{d\psi_j}{dx}dx \tag{2.64}$$

Using this transformation, as in all finite elements, we transform our global stiffness into a local element integral.

$$K_{ij}^e = \int_{-1}^{+1} \left[\frac{d\psi_i}{dr}\frac{dr}{dx}\right]\left[\frac{d\psi_j}{dr}\frac{dr}{dx}\right]\frac{dx}{dr}dr = \int_{-1}^{+1} \frac{d\psi_i}{dr}\frac{d\psi_j}{dr}\frac{dr}{dx}dr \tag{2.65}$$

In our case this integral becomes

$$K_{ij}^e = 4\int_{-1}^{+1} \frac{d\psi_i}{dr}\frac{d\psi_j}{dr}dr \tag{2.66}$$

The right hand side of the equation must also be constructed. This right hand side forcing vector is defined as,

$$F_i^e = \int_{x_l}^{x_r} \psi_i \left[\sin\left(3\pi x\right)\right] dx \tag{2.67}$$

This right hand side will be different for each element.

$$\begin{aligned} F_i^1 &= \frac{1}{4}\int_{-1}^{+1} \psi_i \left[\sin\left(3\pi\frac{r+1}{4}\right)\right] dr \\ F_i^2 &= \frac{1}{4}\int_{-1}^{+1} \psi_i \left[\sin\left(3\pi\frac{r+3}{4}\right)\right] dr \end{aligned} \tag{2.68}$$

We use equation 2.66 to generate the stiffness matrix and equation 2.68 to generate the right hand side vector. Solution for first all the way to sixth order is shown in figure 2.18. For the linear solution notice the solution is exact at the node. This will always occur for linear second order differential equations. Interested readers may consult the text by Reddy [13] for further details. The finite element solution is indiscernible from the exact solution for 5^{th} order up. However, the computational effort involved in the higher order solution amounts to simply calculating the right hand side vector from equation 2.68. The system matrix need not be calculated since it will simply generate a one on the diagonal and zero every where else. As a result, the degrees of freedom associated with the hierarchial degrees of freedom may be obtained by determining the right hand side vector, 2.68. In fact the hierarchial degrees of freedom are equal to the right hand side associate with each hierarchial basis function. Interested readers may consult the Matlab file `GramSchmidtHierarchialStiffness.m` for a complete description of the approach.

Draft
9"
Copyright Dr. R. Fithen

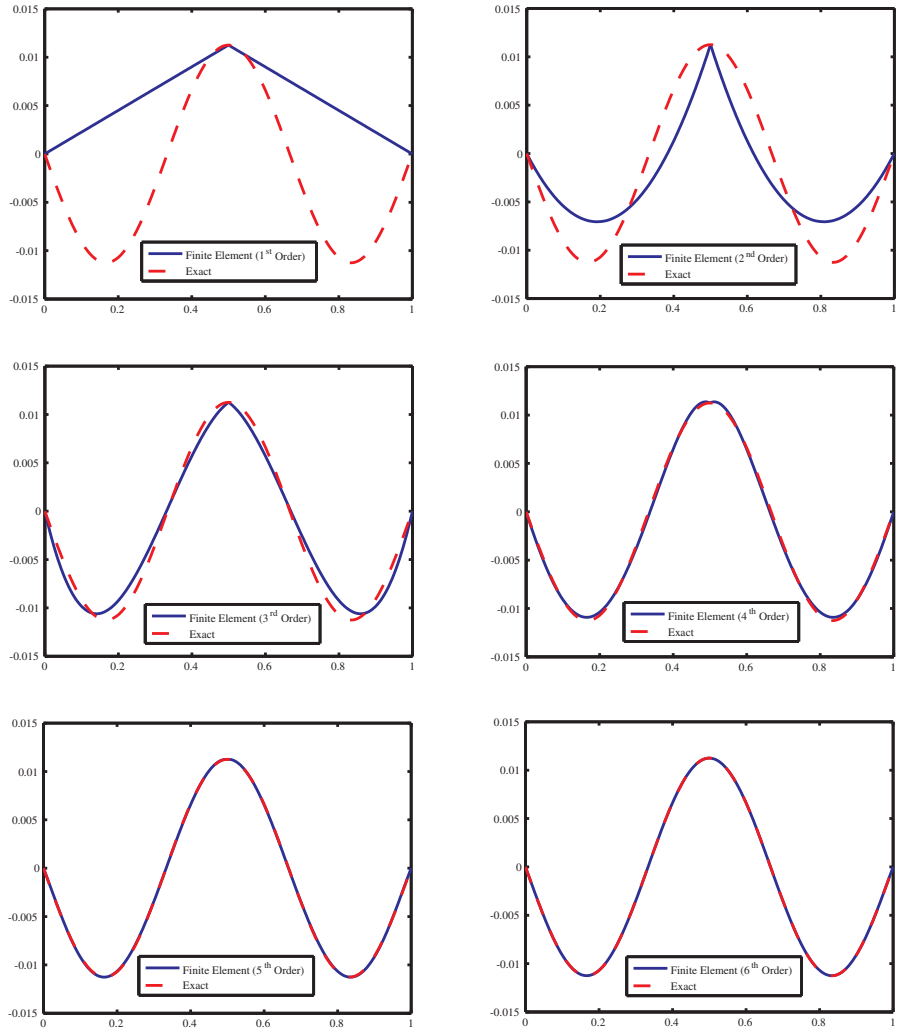


Figure 2.18: Two Element Solution to Test Problem

2.4 Two Dimensional Basis Functions

Our primary task throughout this text deals with two dimensional problems. As a result this section is very pertinent to the topic at hand. The section on one dimensional basis functions is primarily a setup for this section. A smooth transition from one to two dimensional basis functions occur through a tensor product approach. Basis function may be subdivide into two large categories, those for quadrilateral shaped elements and those for triangular shaped elements. We will begin with the quadrilateral element's basis functions.

6"
9"
Draft
Copyright Dr. R. Fithen

2.4.1 Primal Basis Function

All basis function may be mapped to this basis function set. In two dimensions a function may be represented by primal coordinates by a polynomial expressed as shown in equation 2.69.

$$\mathcal{T}(r,s) = \sum_{i=0}^{N_r}\sum_{j=0}^{N_s} a_{ij} r^i s^j \tag{2.69}$$

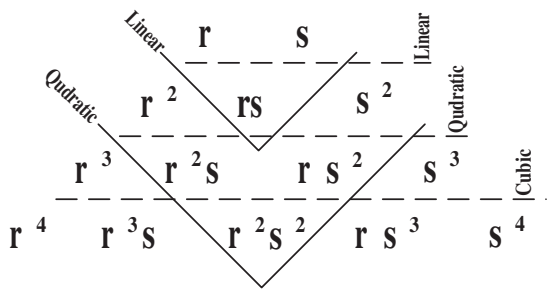


Figure 2.19: Pascal's Triangle

Commonly this primal basis function is written in terms of Pascal's triangle shown in figure 2.19. Down the left of Pascal's triangle the designation for the order of the approximate refers to a quadrilateral element. The order described down the right is that of a triangular element. For a linear quadrilateral element four unknowns are required, a_{00}, a_{10}, a_{01} and a_{11}. As we shall see shortly these unknowns can map directly to four nodal unknowns of the dependent variable. Likewise, a linear triangle requires three unknowns, a_{00}, a_{10} and a_{01}. These too can be directly mapped to our unknown dependent variables. In fact we shall use this mapping as a base point for higher order mappings. As an example, higher order spectral elements may be mapped directly to higher order hierarchial based elements.

2.4.2 Primal to Linear Quadrilateral Mappings

In this section we will show how a transformation matrix may be used to map the polynomial from primal basis to a more useful representation of the same order. This mapping has been used through finite elements for years and is commonly accepted. However, our purpose is to setup a process which we will use later in higher order elements. We begin with a standard quadrilateral element as shown in figure 2.20. Our primal basis function for this linear quadrilateral element is shown in equation 2.70

$$\mathcal{T}(r,s) = a_{00} + a_{10}r + a_{01}s + a_{11}rs \tag{2.70}$$

Using this primal basis functions and the commonly accepted definition in finite elements that the nodes exist at the vertexes of the quadrilateral we obtain a condition shown in equation 2.71.

$$\mathcal{T}(r_i,s_i) = \mathcal{T}_i \qquad \forall \qquad i = 1,2,3,4 \tag{2.71}$$

Draft
Copyright Dr. R. Fithen

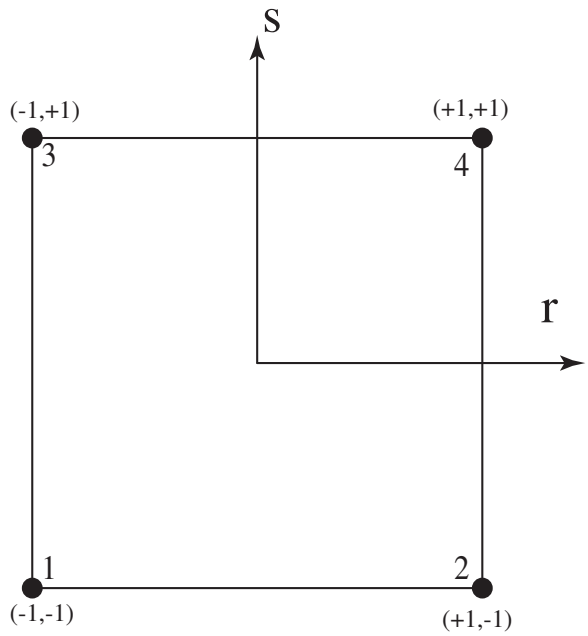


Figure 2.20: Quadrilateral Element

Where x_i and y_i refer to the local nodal numbering system shown in figure 2.20.

$$\begin{aligned}
\mathcal{T}_1 &= \mathcal{T}(-1,-1) = a_{00} - a_{10} - a_{01} + a_{11} \\
\mathcal{T}_2 &= \mathcal{T}(+1,-1) = a_{00} + a_{10} - a_{01} - a_{11} \\
\mathcal{T}_3 &= \mathcal{T}(-1,+1) = a_{00} - a_{10} + a_{01} - a_{11} \\
\mathcal{T}_4 &= \mathcal{T}(+1,+1) = a_{00} + a_{10} + a_{01} + a_{11}
\end{aligned} \tag{2.72}$$

In matrix form these equations become.

$$\begin{pmatrix} \mathcal{T}_1 \\ \mathcal{T}_2 \\ \mathcal{T}_3 \\ \mathcal{T}_4 \end{pmatrix} = \begin{bmatrix} +1 & -1 & -1 & +1 \\ +1 & +1 & -1 & -1 \\ +1 & -1 & +1 & -1 \\ +1 & +1 & +1 & +1 \end{bmatrix} \begin{pmatrix} a_{00} \\ a_{10} \\ a_{01} \\ a_{11} \end{pmatrix} \tag{2.73}$$

Inverting this matrix and solving for the primal coefficients we obtain.

$$\begin{pmatrix} a_{00} \\ a_{10} \\ a_{01} \\ a_{11} \end{pmatrix} = \frac{1}{4} \begin{bmatrix} +1 & +1 & +1 & +1 \\ -1 & +1 & -1 & +1 \\ -1 & -1 & +1 & +1 \\ +1 & -1 & -1 & +1 \end{bmatrix} \begin{pmatrix} \mathcal{T}_1 \\ \mathcal{T}_2 \\ \mathcal{T}_3 \\ \mathcal{T}_4 \end{pmatrix} \tag{2.74}$$

6"
9"
Draft
Copyright Dr. R. Fithen

6"

Inserting a_{ij} from equation 2.74 into equation 2.70 we have equation 2.75.

$$\begin{aligned}\mathcal{T}(r,s) =& \frac{1}{4}(+1-1r-1s+1rs)\,\mathcal{T}_1+\\ & \frac{1}{4}(+1+1r-1s-1rs)\,\mathcal{T}_2+\\ & \frac{1}{4}(+1-1r+1s-1rs)\,\mathcal{T}_3+\\ & \frac{1}{4}(+1+1r+1s+1rs)\,\mathcal{T}_4\end{aligned} \tag{2.75}$$

Observing this equation 2.75 we may write our approximation in terms of standard finite element shape functions. In this case, the standard finite element shape functions are bilinear and may be expressed as shown in equation 2.76.

$$\begin{aligned}\mathcal{T}(r,s) =& \psi_1\mathcal{T}_1+\psi_2\mathcal{T}_2+\psi_3\mathcal{T}_3+\psi_4\mathcal{T}_4\\ =& \frac{1}{4}(1-r-s+rs)\,\mathcal{T}_1+\\ & \frac{1}{4}(1+r-s-rs)\,\mathcal{T}_2+\\ & \frac{1}{4}(1-r+s-rs)\,\mathcal{T}_3+\\ & \frac{1}{4}(1+r+s+rs)\,\mathcal{T}_4\end{aligned} \tag{2.76}$$

From this set of equations we may see our new basis functions emerge as shown in equation 2.77.

$$\begin{aligned}\psi_1 =& \frac{1}{4}(1-r-s+rs) = \frac{1}{4}(1-r)(1-s)\\ \psi_2 =& \frac{1}{4}(1+r-s-rs) = \frac{1}{4}(1+r)(1-s)\\ \psi_3 =& \frac{1}{4}(1-r+s-rs) = \frac{1}{4}(1-r)(1+s)\\ \psi_4 =& \frac{1}{4}(1+r+s+rs) = \frac{1}{4}(1+r)(1+s)\end{aligned} \tag{2.77}$$

Or in matrix form these equations may be written as shown in 2.78. Notice one interesting fact, the transformation matrix in equation 2.78 is the transpose of the transformation matrix shown in equation 2.74.

$$\begin{pmatrix}\psi_1\\ \psi_2\\ \psi_3\\ \psi_4\end{pmatrix} = \frac{1}{4}\begin{bmatrix}+1 & -1 & -1 & +1\\ +1 & +1 & -1 & -1\\ +1 & -1 & +1 & -1\\ +1 & +1 & +1 & +1\end{bmatrix}\begin{pmatrix}1\\ r\\ s\\ rs\end{pmatrix} \tag{2.78}$$

This gives us a transformation matrix from primal basis function to standard bilinear finite element basis functions. This methodology will be used to observe the nature of higher order basis functions. A typical bilinear basis function, along with contours, is shown in figure 2.21. There are four such basis functions which look exactly the same when each is rotated. This figure was produced by the simple Matlab code `BilinearBasisFunction.m`.

Draft
9"
Copyright Dr. R. Fithen

6"

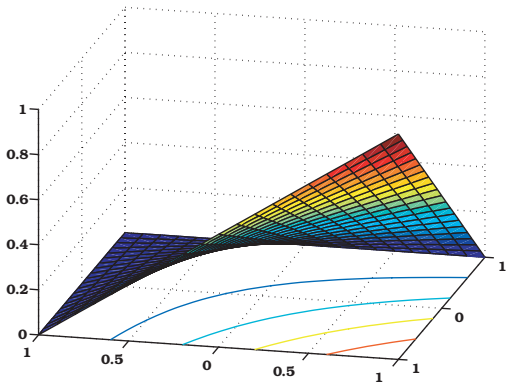


Figure 2.21: Typical Bilinear Basis Function

2.4.3 8-Noded Serendipity Element

In this section we focus primarily on the 8 noded serendipity element. The only reason for inclusion of this element is its use in Stokes equation simulation. The basis function for this element are shown in equation 2.79.

$$\begin{aligned}
\psi_1 &= \frac{1}{4}(1-r)(1-s)(-r-s-1) \\
\psi_2 &= \frac{1}{4}(1+r)(1-s)(+r-s-1) \\
\psi_3 &= \frac{1}{4}(1+r)(1+s)(+r+s-1) \\
\psi_4 &= \frac{1}{4}(1-r)(1+s)(-r+s-1) \\
\psi_5 &= \frac{1}{2}\left(1-r^2\right)(1-s) \\
\psi_6 &= \frac{1}{2}(1+r)\left(1-s^2\right) \\
\psi_7 &= \frac{1}{2}\left(1-r^2\right)(1+s) \\
\psi_8 &= \frac{1}{2}(1-r)\left(1-s^2\right)
\end{aligned} \tag{2.79}$$

Each shape function refers to the nodes as shown in figure 2.5. Expanding and observing term

Draft
9"
Copyright Dr. R. Fithen

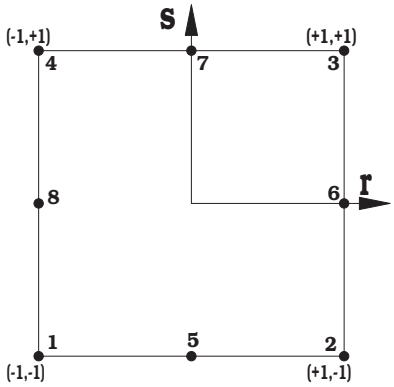


Figure 2.22: Eight noded quadratic serendipity element.

we observe the transformation matrix to the primal basis functions as shown in equation 2.80.

$$\begin{pmatrix}\psi_1\\ \psi_2\\ \psi_3\\ \psi_4\\ \psi_5\\ \psi_6\\ \psi_7\\ \psi_8\end{pmatrix} = \frac{1}{4}\begin{bmatrix} -1 & 0 & 0 & +1 & +1 & +1 & -1 & -1\\ -1 & 0 & 0 & -1 & +1 & +1 & -1 & +1\\ -1 & 0 & 0 & +1 & +1 & +1 & +1 & +1\\ -1 & 0 & 0 & -1 & +1 & +1 & +1 & -1\\ +2 & 0 & -2 & 0 & -2 & 0 & +2 & 0\\ +2 & +2 & 0 & 0 & 0 & -2 & 0 & -2\\ +2 & 0 & +2 & 0 & -2 & 0 & -2 & 0\\ +2 & -2 & 0 & 0 & 0 & -2 & 0 & +2 \end{bmatrix}\begin{pmatrix}1\\ r\\ s\\ rs\\ r^2\\ s^2\\ r^2s\\ rs^2\end{pmatrix} \tag{2.80}$$

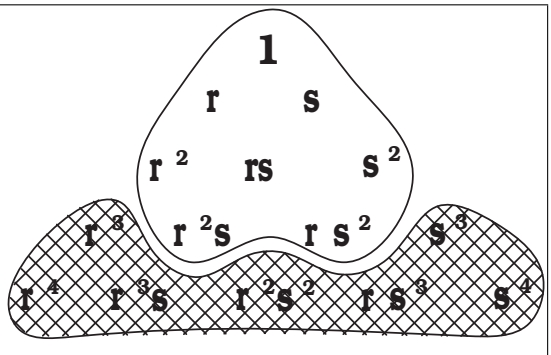


Figure 2.23: Pascal's Triangle

Observing this equation we notice the appearance of every term shown in the clear box in figure 2.23. We notice that the term r^2s^2 is not included. In any basis function construction it is important that the set of functions be complete. In this case our set of functions is indeed complete. If however, our set of functions did not included, for example, the r term in Pascal's triangle then this set would have been incomplete. A plot of these functions is shown in figure 2.24.

6" 9" Draft
Copyright Dr. R. Fithen

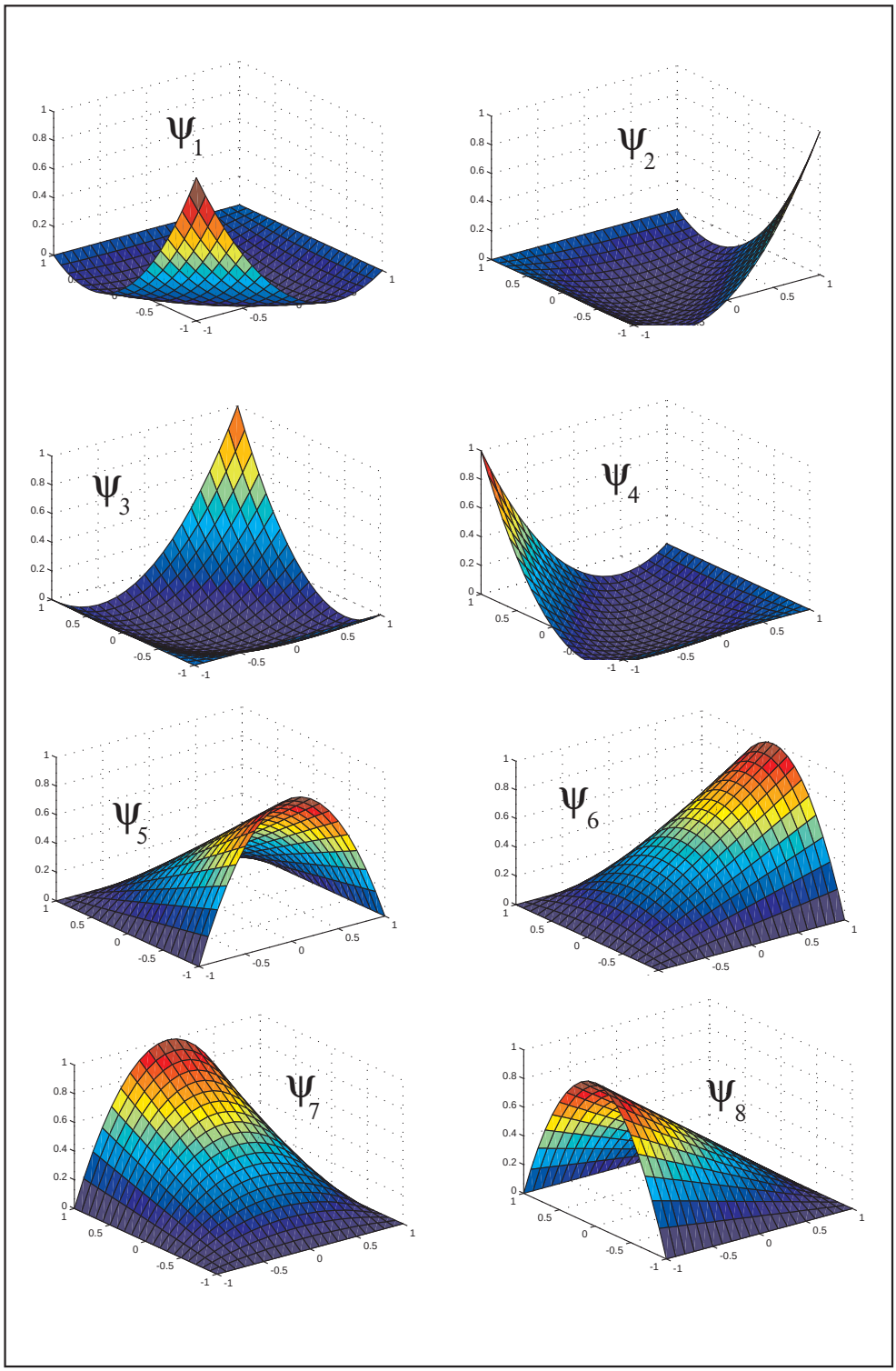


Figure 2.24: Basis functions for 8-noded Serendipity element.

6"
9"
Draft
Copyright Dr. R. Fithen

2.4.4 Two Dimensional Tensor Product Functions

In this section we look at elements basis functions which may be derived from a tensor product approach. Two dimensional tensor product type elements may be developed as shown below in equation 2.81.

$$\phi_{ij}(r,s) = \psi_i(r)\,\psi_j(s) \tag{2.81}$$

Where $\psi_i(r)$ is a one dimensional basis function of a Lagrange, Spectral Lagrange or any of our Hierarchial type basis functions. We begin with our standard equal-distant Lagrange type elements. Since the linear basis function set for of this approach turns out the basis function set shown in equation 2.77, we will begin with a quadratic basis function. Looking closely at equation 2.81 an figure 2.25 we see how the indices relate to our node numbers.

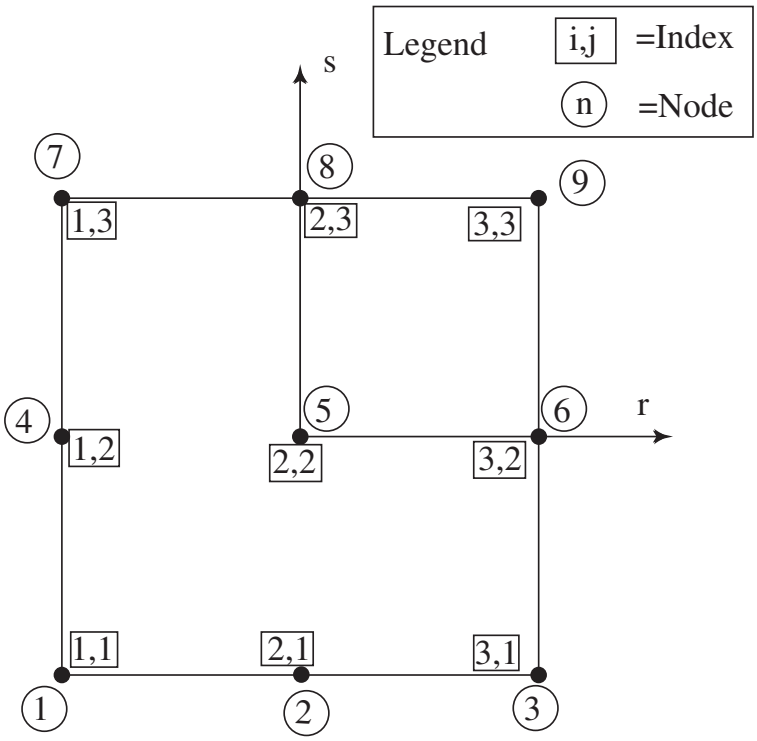


Figure 2.25: Quadratic Basis Function

If our polynomial order is N then we may easily determine the node number as a function of the summation indices i and j. This relationship is shown below in equation 2.82

$$n = (N+1)(j-1) + i \tag{2.82}$$

Where i and j are the indices in equation 2.81 and figure 2.25. This equation, 2.82, can be used for all orders and all types of tensor product type elements. Of course we shall use this numbering scheme throughout the rest of this text. For the quadratic element a plot of the nine basis functions is shown in figure 2.26.

6"
9"
Draft
Copyright Dr. R. Fithen

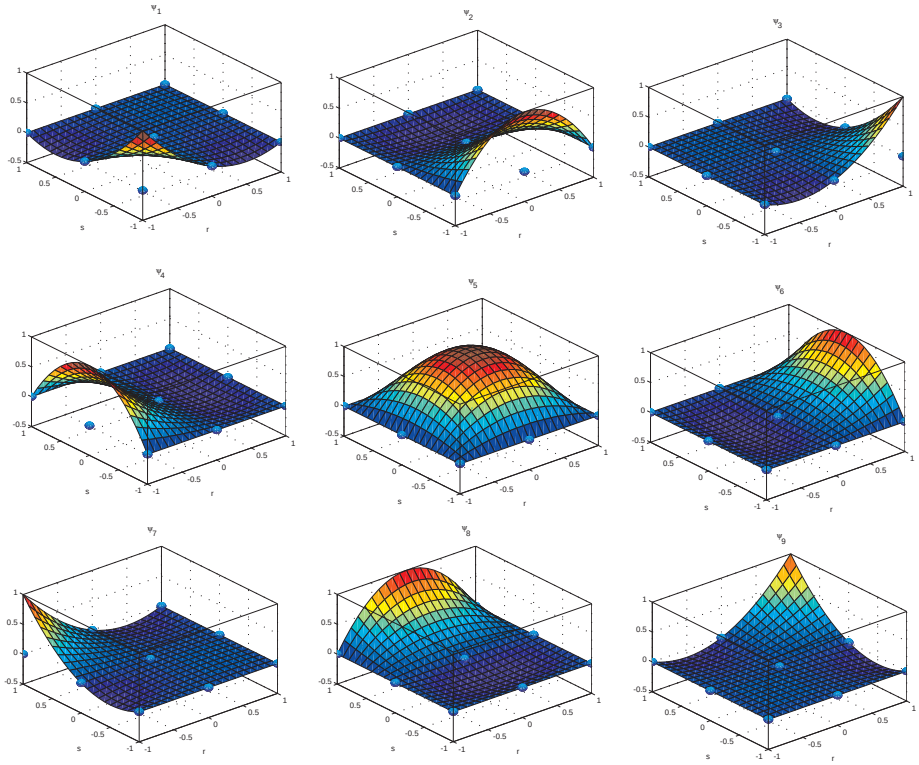


Figure 2.26: Quadratic Lagrange Elements

Notice the appearance of small spheres in this plot. These spheres are nodes placed on the plots for reference. For spectral elements the only difference is the nodal placement. Since, the differences is seen at higher order we only show a few basis functions of the 49 possible functions for a 6^{th} order element. A selected number of these functions are shown in figure 2.27. Notice the clustering of nodes towards the edges of the elements. This is a result of the use of equation 2.23 in the one dimensional element construction. Since all information is brought into multi dimensions through the tensor product, nodal placement is exactly the same as in the one dimensional case.

For Lagrange elements, both equal-distant and spectral placement, each node is associated very closely with the basis functions. In fact, the basis functions are of value one at their associated node and zero at all other nodes. This requirement add significance to the solution of our problem. The unknowns expressed in an expansion, equation 2.83, are the actual values at the specific node where the basis function is unity.

$$T(r,s) = \sum_{i=1}^{N}\sum_{j=1}^{N} T_{ij}\phi_{ij}(r,s) \tag{2.83}$$

Copyright Dr. R. Fithen

6"

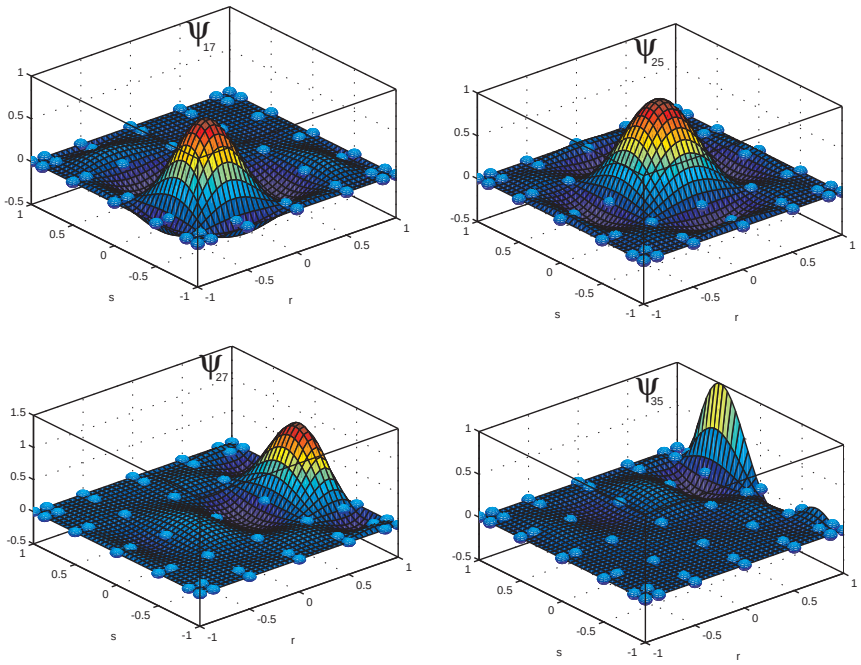


Figure 2.27: Spectral Elements

This convenient property that exist in Lagrange type elements is given up for hierarchial. We are not willing to give up this property without just cause. Hierarchial elements, as we have seen in one dimension, possess a important property. This property exist within the multi dimensional hierarchial element as well. Hierarchial elements are capable of increased polynomial telescoping. This means that while increasing to a polynomial order of M all previous basis functions from order 1 to $(M-1)$ all remain intact. As a result all element matrices, mass and stiffness, possess an embedding property. All element matrices of order M have embedded within them the matrices of all lower order, 1 to $(M-1)$. We have also seen that a Gram-Schmidt orthonormalization will give a very nice property in one dimension. The question one may ask is: Is this orthonormalization possible in multi dimensions? To answer this question we must first construct our tensor product and only then can we work our basis functions into a orthonormal basis. This is the subject matter of the next subsection.

2.4.5 Hierarchial Orthonormal Basis Functions (Mass Based)

In this subsection we seek orthonormal hierarchial basis functions. These functions will be tensor products of one dimensional functions. However, the nodal number scheme will be altered to separate the different type of nodal degrees of freedom. In Lagrange type elements each node is associate with a specific basis function. The relationship between the node and

Draft
9"
Copyright Dr. R. Fithen

6"

basis function is very important in Lagrange type elements. As we have seen previously the

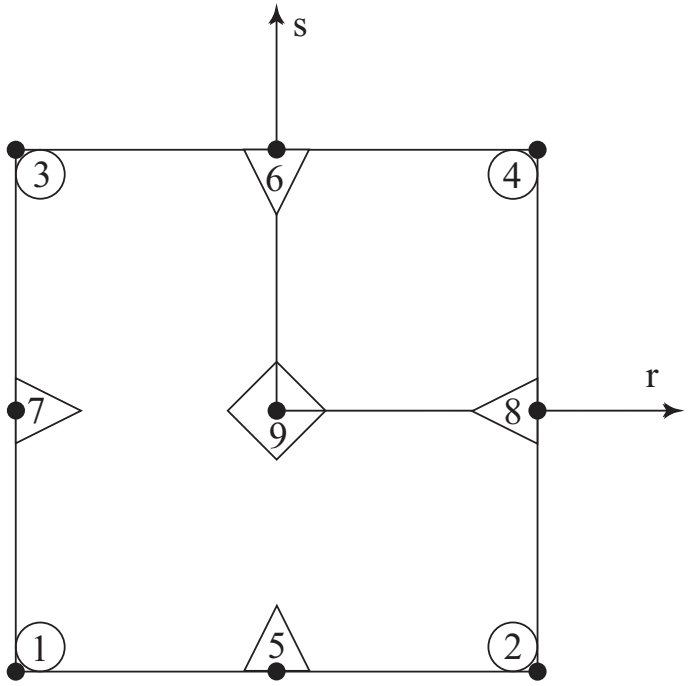


Figure 2.28: Hierarchial Element Nodes

there is only one node in which the basis function's value is unity, all other nodes the function's value is zero. However, in hierarchial basis functions this is not the case. The higher order functions, quadratic and higher, have no relationship with any nodal location within the element. One may force this type relationship based on the derivative of the approximation, much like a hermite type of element. We will take this approach since our goal will always be to force our higher order basis function set to be orthonormal to each other. With all of this information in mind we must determine a nodal structure for our hierarchial elements, figure 2.28. In this figure we see the vertices of the quadrilateral, in circles, are numbered first followed by the side nodes, in triangles, and the center node, in a diamond. The first four nodes have one degree of freedom each associated with them. In fact the first for basis functions are exactly the same as the bilinear basis functions shown in equation 2.77 and figure 2.18. The side nodes have several interesting properties. First, these nodes have no particular location in the same manner a Lagrange node would. In other words, there is no basis function which has its value as unity along the side as in the Lagrange type elements. In addition, there exist $O-1$ basis functions associated with this side node, where O is the polynomial order of the approximation. The internal node, 9^{th} node, has the same general behavior as the side. However, there are $(O-1)^2$ basis function associated with this node. A plot of the bilinear basis functions along with the side node degree of freedoms are shown in figure 2.29. The basis functions shown in this figure are created from the tensor products of

Draft
9"
Copyright Dr. R. Fithen

6"

the mass based one dimensional basis functions, see equation 2.53.

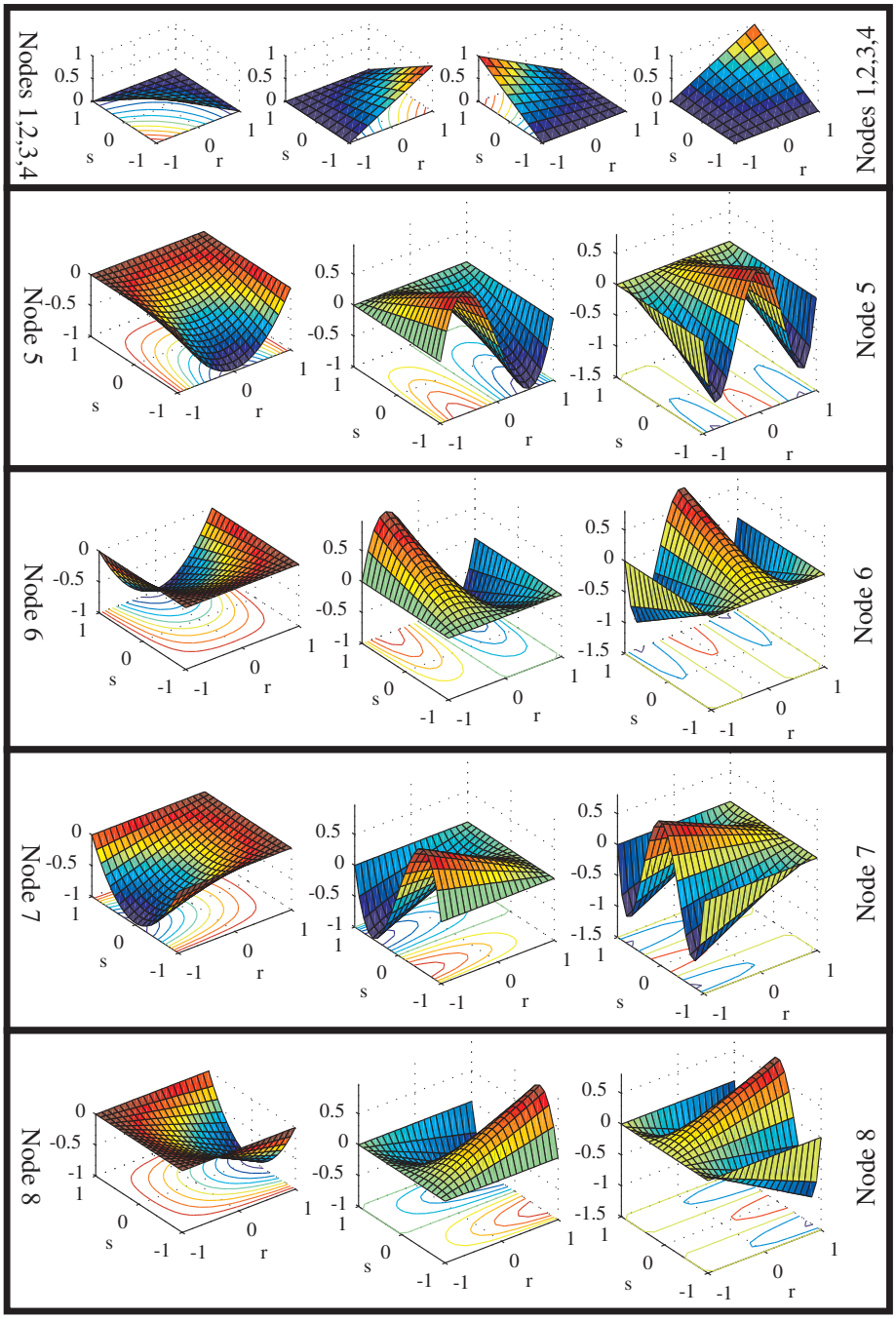


Figure 2.29: Basis functions for Vertices and Side Nodes (4^{th} Order Mass Based).

Draft
9"
Copyright Dr. R. Fithen

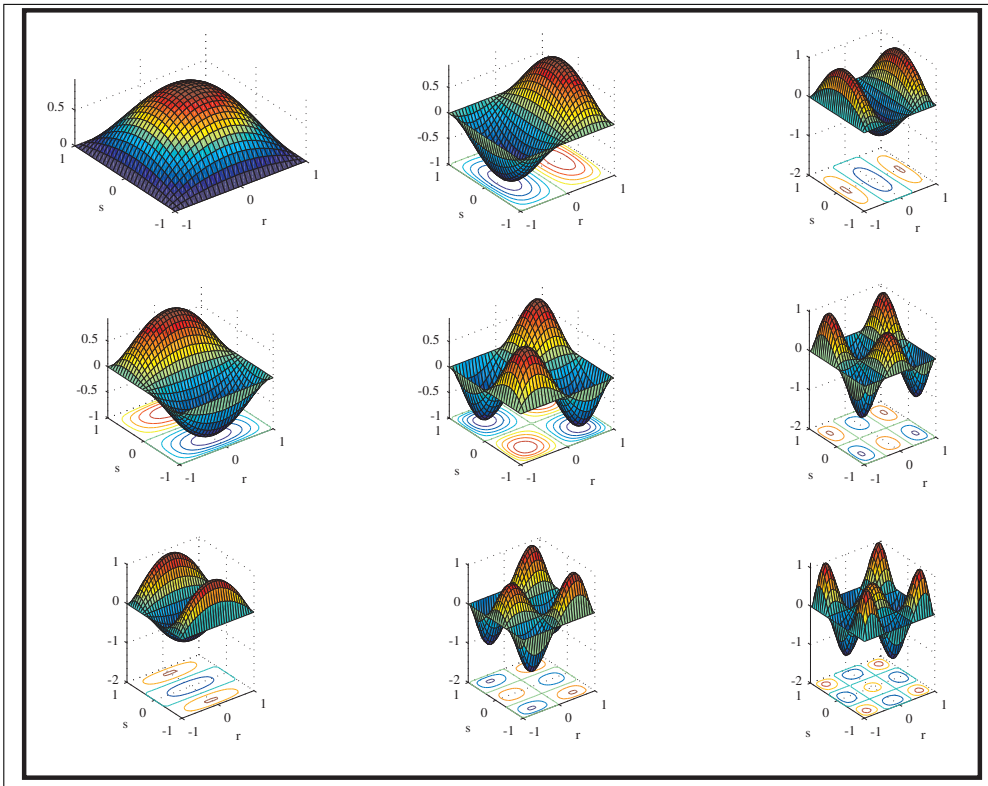


Figure 2.30: Basis functions for Internal Nodes (4^{th} Order Mass Based).

Order	Side DOFs	Internal DOFs
1	0	0
2	1	1
3	2	4
4	3	9
5	4	16
6	5	25
7	6	36
8	7	49
9	8	64
10	9	81
11	10	100
12	11	121

Table 2.1: Basis Function Degrees of Freedom

These plots represent a 4^{th} order hierarchial basis function set. As a result, there are 3 degrees of freedom, basis functions, associated with each side node. The internal nodes are

6"
9"
Draft
Copyright Dr. R. Fithen

6"

shown in figure 2.30. In this figure we see 9 degrees of freedom, basis functions, associate with node number 9. It does not take long to realize how quickly the number of internal degrees of freedoms increase relative to the side nodes. Table 2.1 shows this up to a 12^{th} order element. As a result of this any element 6^{th} order or higher has more degrees of freedom internal to the element than external. As a result the concept of condensing the internal degrees of freedom become somewhat attractive, especially in higher dimensions. With this in mind, our Gram-Schmidt orthonormalization process is attractive. By performing this process on our hierarchial basis function set we will obtain the identity matrix associated with the internal basis functions.

As it turns out, our basis functions are already orthonormal with respect to our mass matrix. This occurs as a result of the mass matrix symmetry with respect to our coordinates.By observing the two dimensional mass matrix as shown in equation 2.84

$$M_{l,k} = \int_{-1}^{+1} \int_{-1}^{+1} \varphi_l(r,s)\, \varphi_k(r,s)\, drds \tag{2.84}$$

Where:

$$\varphi_{n(i,j)}(r,s) = \psi_i(r)\, \psi_j(s) \tag{2.85}$$

Where the relationship between i, j and n is shown as a functional relationship as shown above in equation 2.85. Gathering the relationship we obtain the following equation, 2.86

$$M_{l(i,j),k(e,f)} = \int_{-1}^{+1} \int_{-1}^{+1} \psi_i(r)\, \psi_j(s)\, \psi_e(r)\, \psi_f(s)\, drds \tag{2.86}$$

Or:

$$M_{l(i,j),k(e,f)} = \int_{-1}^{+1} \left(\int_{-1}^{+1} \psi_i(r)\, \psi_e(r)\, dr \right) \psi_j(s)\, \psi_f(s)\, ds \tag{2.87}$$

Or:

$$M_{l(i,j),k(e,f)} = \left[\int_{-1}^{+1} \psi_i(r)\, \psi_e(r)\, dr \right] \left[\int_{-1}^{+1} \psi_j(s)\, \psi_f(s)\, ds \right] \tag{2.88}$$

Or:

$$M_{l(i,j),k(e,f)} = \left[M_{ie}^{1D} \right] \left[M_{jf}^{1D} \right] \tag{2.89}$$

From this equation we may surmise that any basis function which is orthonormal in one dimension will also be orthonormal in two dimensions. However, this may not be the case of we wish to force our basis function to be orthonormal with respect to our stiffness matrix. Later we will use Gram-Schmidt orthonormalization with respect to a stiffness matrix on a two dimensional problem. For now we will focus on the matrix structure for our mass matrix. For a 10^{th} order basis function our mass matrix is shown in figure 2.31. It is immediately apparent that our mass matrix has a structure which may be taken advantage of through use of special matrix solvers.

Draft
9"
Copyright Dr. R. Fithen

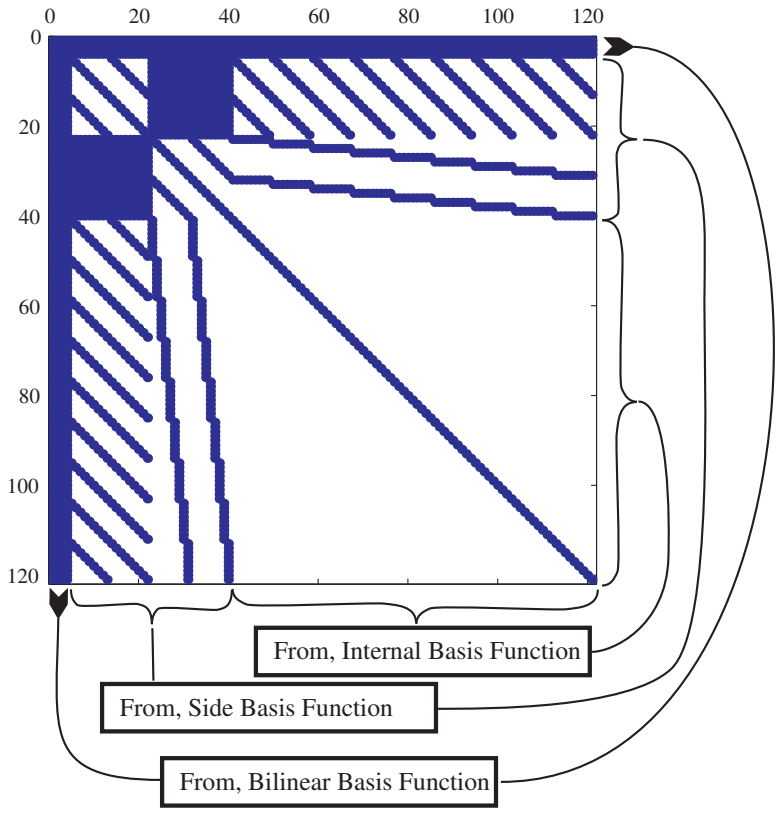


Figure 2.31: Mass Matrix for 10^{th} order basis functions

Although we shall take limited advantage of this matrix structure, it is worth noticing a few properties of this matrix. First and foremost the sub-matrix generated from the internal basis function is the identity matrix. This is by design since we did not want to take the inverse of this sub-matrix. Another observation is there is no special structure with respect to the original bilinear basis function and all side and internal basis functions. In simpler terms this section of the matrix, across the top and down the left most side, is fully populated. However, the does appear to be a structure to the side basis functions portion of the matrix. To understand this we look back at figures 2.28 and 2.29. Looking at our nodal number scheme for our side and our basis functions for those node we see a pattern emerge. Basis functions associate with nodes 5 and 6 have a interesting dependency with respect to our mass matrix. The first degree of freedom, basis function, associate with node 5 is orthogonal to all degrees of freedom, basis functions, associated with node 6 with one exception. The first degree of freedom associate with node 5 is not orthogonal to the first degree of freedom associate with node 6. Remember, our two dimensional mass matrix integrations may be broken into two separable one dimensional integrals as in equation 2.88. Likewise, the second degree of freedom associate with node 5 is not orthogonal to the second degree of freedom associate with node 6. However, the second degree of freedom associate with node 5 is

6"
9"
Draft
Copyright Dr. R. Fithen

6"

orthogonal to every other degrees of freedom associate with node 6. This pattern is observable in the cropped version of the matrix shown in figure 2.32. We can see this structure existing in the matrix construction itself, equation 2.88. Both nodes 5 and nodes 6 contain the bilinear portion of the basis function in the s coordinate and the hierarchial portion in the r coordinate direction, see figure 2.29. As a result, the bilinear portion of the integration, $\int_{-1}^{+1} \psi_j(s)\,\psi_f(s)\,ds$ in equation 2.88, simply adds a scaling factor. The hierarchial portion of the basis function, $\int_{-1}^{+1} \psi_i(r)\,\psi_e(r)\,dr$ in equation 2.88, is by definition orthonormal. Keeping this mentality, we may easily see how the matrix structure for the dark portion shown in figure This full sub-matrix is a result of the interaction between the linear portion of the basis function and the hierarchial portion of 2.33. the basis function. For example, the interaction between node 5 and node 7 generates a full sub-matrix. This occurs because the one dimensional portion of the integration, $\int_{-1}^{+1} \psi_i(r)\,\psi_e(r)\,dr$ in equation 2.88, is an interaction between the linear portion of the basis function and the hierarchial portion of the basis function.

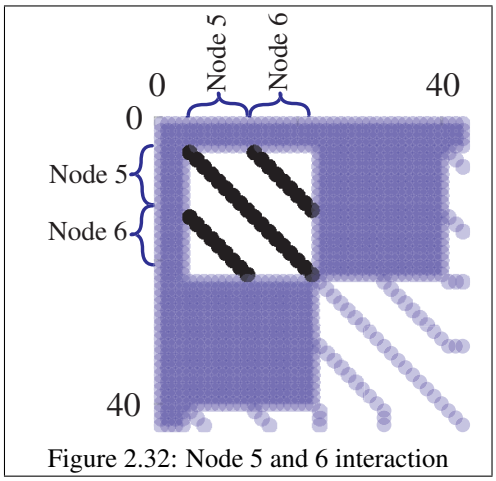


Figure 2.32: Node 5 and 6 interaction

We could carry out a similar analysis throughout every portion of the matrix. However, not every matrix will shown the same structure. For this reason, we will move on to look at the structure of the stiffness matrix. Of course, the construction of the stiffness matrix is dependent on the differential equation being solved. As a result, many times the use of orthonormal one dimensional basis function offer no simplification to the matrix structure. In fact, in many cases we will have to perform a Gram-Schmidt orthonormalization on our two dimensional basis function set to obtain the identity matrix with respect to our internal basis functions.

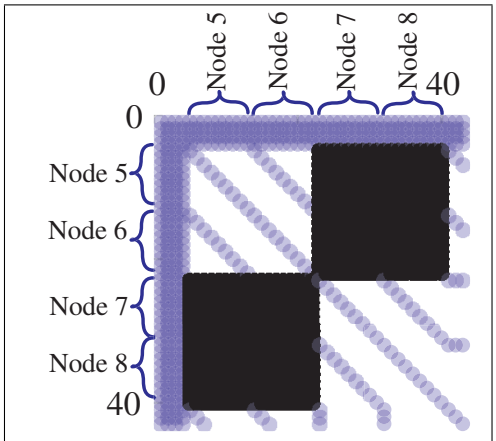


Figure 2.33: Node 5, 6, 7 and 8 interaction

2.4.6 Hierarchial Orthonormal Basis Functions (Stiffness Based)

In this section we will look at a specific stiffness matrix construction. Unlike the mass based orthonormal matrix construction, the stiffness matrix is a direct function of the differential equation being solved. As a result, each differential equation will generate a different orthonormal basis function set. In this section we will focus on using the Laplace type equations. These equations are commonly seen in conduction heat transfer, flow through porous media, electro statics, as well as many other applications. We shall look at the isotropic version of

Draft
9"
Copyright Dr. R. Fithen

6"

this equation as shown in the equation below.

$$\frac{\partial^2 T}{\partial r^2} + \frac{\partial^2 T}{\partial s^2} = Q_f \tag{2.90}$$

It may be tempting at first to use a tensor product of the basis functions generated for the one dimensional orthonormal stiffness matrix, equation 2.56. Doing so will yield a matrix as shown in figure 2.34.

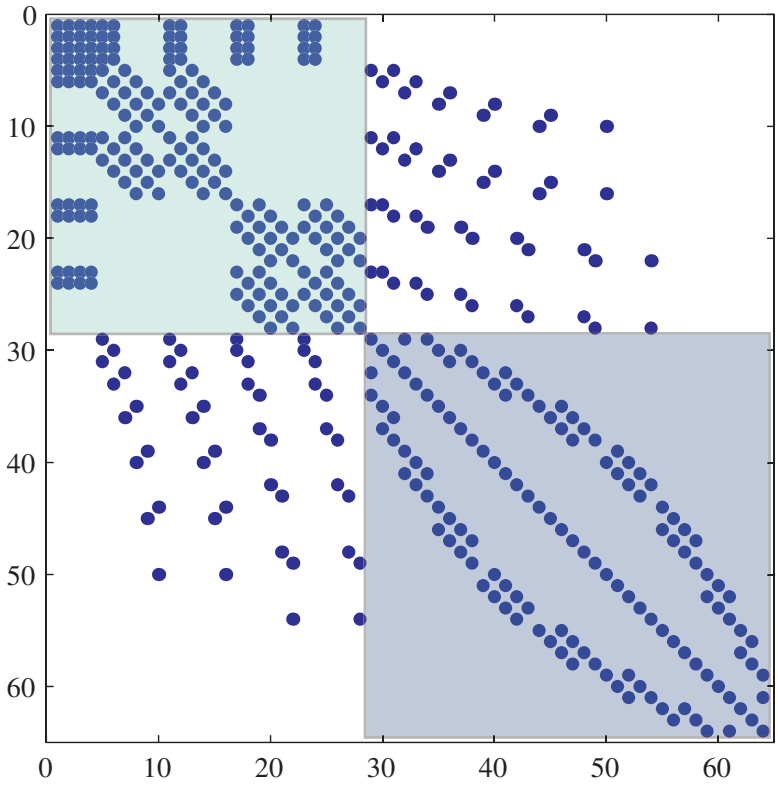


Figure 2.34: Stiffness Matrix for 7^{th} order basis functions

In this figure the shaded area at the lower right represents the submatrix associated with the internal degrees of freedom, node 9. Our goal with respect to this submatrix is its conversion to the identity matrix. It is obvious that blind use of the tensor product of the basis functions from equation 2.56 does not accomplish this. By looking at how the stiffness matrix is defined and how our tensor product is defined we will see why an orthonormal one dimensional basis functions do not translate into orthonormal two dimensional basis functions. Our stiffness matrix is defined by equation 2.92 below.

$$K_{nm} = \int_{-1}^{+1} \int_{-1}^{+1} \left(\frac{\partial \varphi_n}{\partial r} \frac{\partial \varphi_m}{\partial r} + \frac{\partial \varphi_n}{\partial s} \frac{\partial \varphi_m}{\partial s} \right) dr ds \tag{2.91}$$

Draft
9"
Copyright Dr. R. Fithen

6"

Where:

$$\varphi_{n(i,j)}(r,s) = \psi_i(r)\,\psi_j(s) \tag{2.92}$$

Where the relationship between i, j and n is shown as a functional relationship. Gathering the relationship we obtain the following equation, 2.86

$$K_{n(i,j),m(e,f)} = \int_{-1}^{+1}\int_{-1}^{+1}\left(\frac{d\psi_i(r)}{dr}\psi_j(s)\frac{d\psi_e(r)}{dr}\psi_f(s) + \psi_i(r)\frac{d\psi_j(s)}{ds}\psi_e(r)\frac{d\psi_f(s)}{ds}\right)drds \tag{2.93}$$

Or, without the independent variables listed:

$$K_{nm} = \int_{-1}^{+1}\int_{-1}^{+1}\left(\frac{d\psi_i}{dr}\frac{d\psi_e}{dr}\psi_j\psi_f + \frac{d\psi_j}{ds}\frac{d\psi_f}{ds}\psi_i\psi_e\right)drds \tag{2.94}$$

Or:

$$\begin{aligned} K_{nm} = &\int_{-1}^{+1}\psi_j\psi_f\left(\int_{-1}^{+1}\frac{d\psi_i}{dr}\frac{d\psi_e}{dr}dr\right)ds \\ &+\int_{-1}^{+1}\psi_i\psi_e\left(\int_{-1}^{+1}\frac{d\psi_j}{ds}\frac{d\psi_f}{ds}ds\right)dr \end{aligned} \tag{2.95}$$

Or:

$$\begin{aligned} K_{nm} = &\left[\int_{-1}^{+1}\psi_j\psi_f ds\right]\left[\int_{-1}^{+1}\frac{d\psi_i}{dr}\frac{d\psi_e}{dr}dr\right] \\ &+\left[\int_{-1}^{+1}\psi_i\psi_e dr\right]\left[\int_{-1}^{+1}\frac{d\psi_j}{ds}\frac{d\psi_f}{ds}ds\right] \end{aligned} \tag{2.96}$$

In order for these basis functions to generate an identity matrix K_{nm} must equal 0 when $n \neq m$. However, when $n \neq m$ there does exist the situation that $i = e$ or $j = f$. In that case, the off diagonal term will not be zero. This is exactly what happens in our case. As a result, we must perform the Gram-Schmidt orthonormalization on these internal degrees of freedom. Performing Gram-Schmidt orthonormalization on the basis functions associated with node nine yields a new stiffness matrix, shown in figure 2.35. From this figure we immediately notice our submatrix in the lower right hand portion of the full matrix is diagonal. In fact this submatrix is the identity matrix generate from our orthonormal basis functions. Another feature noticable in figures 2.34 and 2.35 is the upper shaded submatrix. This portion of the matrices is exactly the same as the upper shaded section of figure 2.34. This is beacuse we did not alter any basis functions associated with nodes 1 through 8. However, the unshaded portions from figures 2.34 and 2.35 are different. This difference is due to our alteration of the internal basis functions thereby changing the interaction between node 9 and all other nodes in the element.

Draft
9"
Copyright Dr. R. Fithen

6"

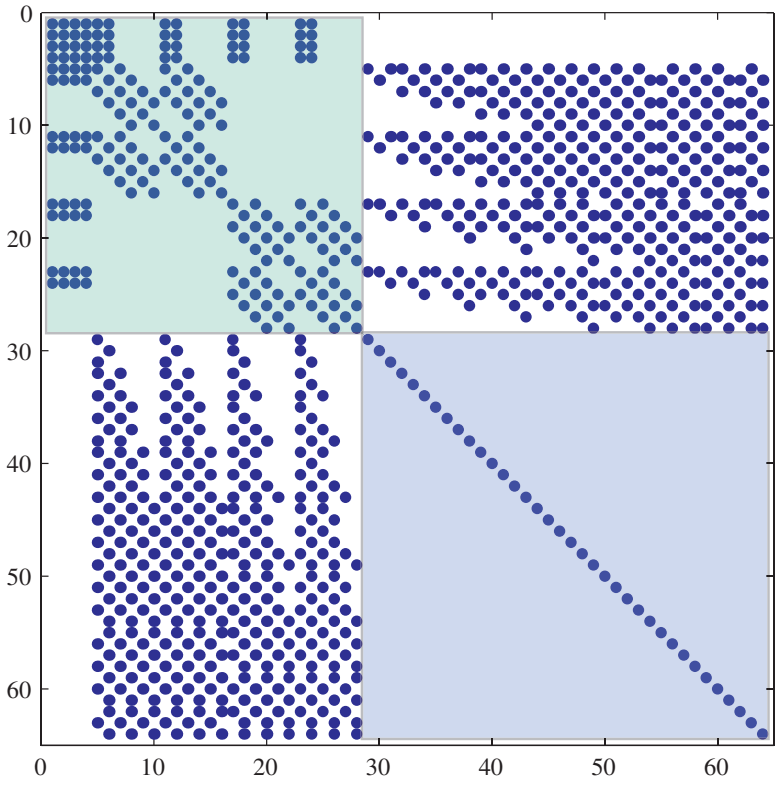


Figure 2.35: Stiffness Matrix for 7^{th} order basis functions

Any element matrix with a structure shown in figure 2.35 lends itself to a substructuring method. Element matrices can be represented as

$$\begin{bmatrix} K_{11} & K_{12} \\ K_{21} & I \end{bmatrix} \begin{pmatrix} T_1 \\ T_2 \end{pmatrix} = \begin{pmatrix} F_1 \\ F_2 \end{pmatrix} \tag{2.97}$$

Expanding these equations we have

$$\begin{aligned} K_{11}T_1 + K_{12}T_2 &= F_1 \\ K_{21}T_1 + T_2 &= F_2 \end{aligned} \tag{2.98}$$

Substituted and eliminating all the internal degrees of freedom yields a matrix equation,

$$[K_{11} - K_{12}K_{21}]\, T_1 = F_1 - K_{12}F_2 \tag{2.99}$$

Eliminating the internal degrees of freedom the matrix structure is shown in figure 2.36.

9"
Draft
Copyright Dr. R. Fithen

6"

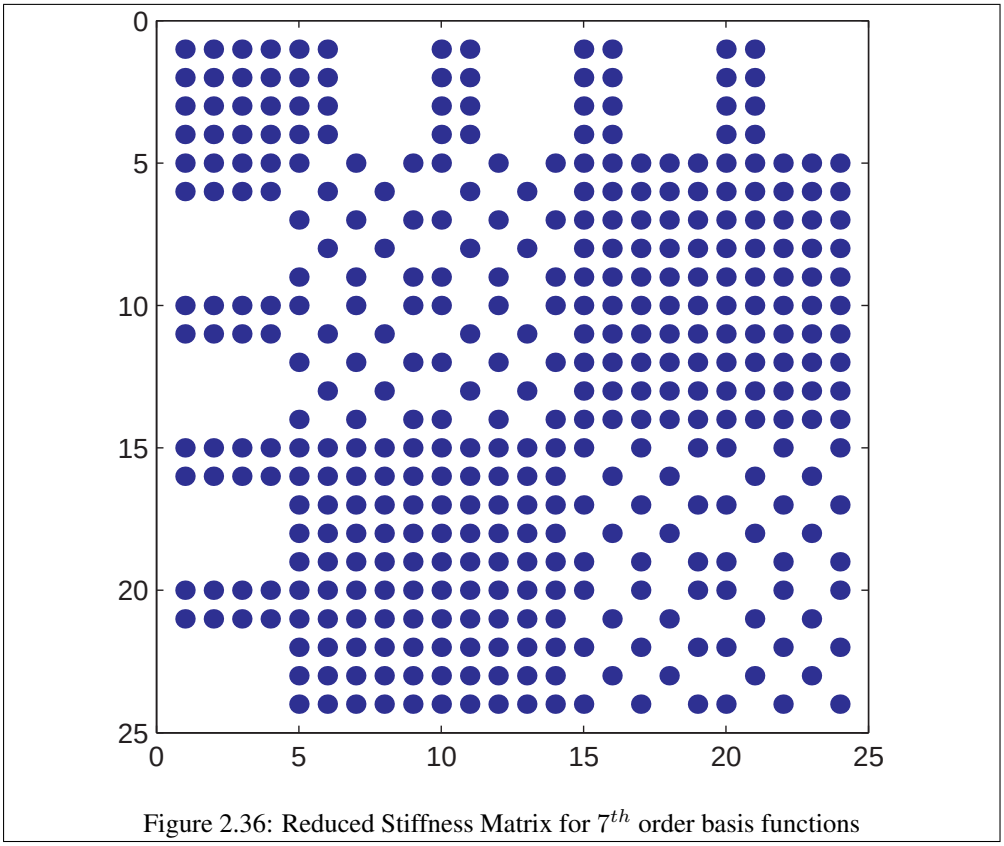


Figure 2.36: Reduced Stiffness Matrix for 7^{th} order basis functions

As we can see using Gram-Schmidt on the internal degrees of freedom will indeed reduce the amount of computational effort required to produce a simulation by reducing the number of unknowns in the direct calculation. Once the calculation is performed each element's internal degrees of freedoms will be individually calculated using the bottom equation in equation 2.100, shown below.

$$T_2 = F_2 - K_{21}T_1 \tag{2.100}$$

Where T_1 is the degrees of freedom for the side nodes and corner nodes (bilinear).

It would be especially convenient if in fact all the side and internal nodes that are added to a bilinear element produced a identity matrix, or at least a diagonal matrix. As we have seen in the sections on one dimensional basis functions this could be done by both a Gram-Schmidt process or a eigenvector analysis. As we have seen in these one dimensional sections eigenvector analysis produced non unique basis functions which were not hierarchial. However, if we decide that an adaptive solution is not needed this approach is acceptable. In the next section we take this approach to investigate whether this type of basis function could be developed.

9"
Draft
Copyright Dr. R. Fithen

6"
9"
Draft

Chapter 3

Mixed Formulation

In this chapter we look closely at how Navier-Stokes, as well as Stokes, equations are cast into a weighted residual method. This chapter is written with the assumption that the reader is somewhat familiar with the weighted residual methods. For more details on the weighted residual methods readers may consult [13] and [**?**].

3.0.7 Mixed Stokes equations

In this section we consider the weighted residual formulation for Stokes equations. Following the standard weighted residual approach we integrate Stokes equations over the domain against a test function. Looking at the weighted residual statement, equation 3.1, we see our weighting term w_j and our residual $\mathcal{R}\left(c_1, c_2, \cdots c_n\right)$ must be orthogonal to each other. The terms, $c_1, c_2, \cdots c_n$ are the constants we wish to determine from this analysis. once these terms are found we have an approximate solution to our equation.

$$\int_{\mathcal{D}} w_j \mathcal{R}\left(c_1, c_2, \cdots c_n\right) d\mathcal{D} = 0 \qquad \forall \qquad j = 1, 2, \cdots n \tag{3.1}$$

The weighting function w_j is may be any set of functions at this point. However, these functions must be linearly independent. A typical case of linear independence may be expressed as in equation 3.2.

$$w_4 \neq a_1 w_1 + a_2 w_2 + a_3 w_3 \tag{3.2}$$

In words, there are no constants a_1, a_2, a_3 such that w_4 may be written as a linear combination of w_1, w_2, w_3. Details of these formulations and approaches may be seen in [13].

We begin by looking closely at the unconstrained Navier-Stokes equations, **??** - **??**. For the present we will exclude the energy equation from consideration. In addition, we will drop the acceleration term, which will result in Stokes equations. Casing these equations into a weighted residual form we obtain equations .

Copyright Dr. R. Fithen

Weighted Residual Formulation of Unreduced Stokes Equations

Continuity:

$$\int_x \int_y w_p \left[\frac{\partial u}{\partial x} + \frac{\partial v}{\partial y} \right] dydx = 0 \tag{3.3}$$

X-Momentum:

$$\int_x \int_y w_u \left[\rho \frac{\partial u}{\partial t} - \rho g_x - \frac{\partial}{\partial x} \left[2\mu \frac{\partial u}{\partial x} \right] - \frac{\partial}{\partial y} \left[\mu \left(\frac{\partial u}{\partial y} + \frac{\partial v}{\partial x} \right) \right] + \frac{\partial p}{\partial x} \right] dydx = 0 \tag{3.4}$$

Y-Momentum:

$$\int_x \int_y w_v \left[\rho \frac{\partial v}{\partial t} - \rho g_y - \frac{\partial}{\partial x} \left[\mu \left(\frac{\partial u}{\partial y} + \frac{\partial v}{\partial x} \right) \right] - \frac{\partial}{\partial y} \left[2\mu \frac{\partial v}{\partial y} \right] + \frac{\partial p}{\partial y} \right] dydx = 0 \tag{3.5}$$

In a parallel development we case our reduced Stokes equations into weighted residual form as shown in equations .

Weighted Residual Formulation of Reduced Stokes Equations

Continuity:

$$\int_x \int_y w_p \left[\frac{\partial u}{\partial x} + \frac{\partial v}{\partial y} \right] dydx = 0 \tag{3.6}$$

X-Momentum:

$$\int_x \int_y w_u \left[\rho \frac{\partial u}{\partial t} - \rho g_x - \mu \left(\frac{\partial^2 u}{\partial x^2} + \frac{\partial^2 u}{\partial y^2} \right) + \frac{\partial p}{\partial x} \right] dydx = 0 \tag{3.7}$$

Y-Momentum:

$$\int_x \int_y w_v \left[\rho \frac{\partial v}{\partial t} - \rho g_y - \mu \left(\frac{\partial^2 v}{\partial x^2} + \frac{\partial^2 v}{\partial y^2} \right) + \frac{\partial p}{\partial y} \right] dydx = 0 \tag{3.8}$$

After an integration by parts on each of these formulations we have the unreduced equation set shown in equations .

6" 9" Draft
Copyright Dr. R. Fithen

6"

Weighted Residual Formulation of Unreduced Stokes Equations

Continuity:

$$\int_x \int_y w_p \left[\frac{\partial u}{\partial x} + \frac{\partial v}{\partial y} \right] dydx = 0 \tag{3.9}$$

X-Momentum:

$$\begin{aligned} \int_x \int_y \left[w_u \rho \frac{\partial u}{\partial t} - \rho w_u g_x + \frac{\partial w_u}{\partial x} \left(2\mu \frac{\partial u}{\partial x} - p \right) + \mu \frac{\partial w_u}{\partial y} \left(\frac{\partial u}{\partial y} + \frac{\partial v}{\partial x} \right) \right] dydx \\ = \oint w_u \left[\underbrace{\left(2\mu \frac{\partial u}{\partial x} - p \right)}_{\sigma_{xx}} n_x + \underbrace{\mu \left(\frac{\partial u}{\partial y} + \frac{\partial v}{\partial x} \right)}_{\sigma_{xy}} n_y \right] d\mathcal{S} \end{aligned} \tag{3.10}$$

Y-Momentum:

$$\begin{aligned} \int_x \int_y \left[w_v \rho \frac{\partial v}{\partial t} - \rho w_v g_y + \mu \frac{\partial w_v}{\partial x} \left(\frac{\partial u}{\partial y} + \frac{\partial v}{\partial x} \right) + \frac{\partial w_v}{\partial y} \left(2\mu \frac{\partial v}{\partial y} - p \right) \right] dydx \\ = \oint w_v \left[\underbrace{\left(2\mu \frac{\partial v}{\partial y} - p \right)}_{\sigma_{yy}} n_y + \underbrace{\mu \left(\frac{\partial u}{\partial y} + \frac{\partial v}{\partial x} \right)}_{\sigma_{xy}} n_x \right] d\mathcal{S} \end{aligned} \tag{3.11}$$

Notice in equations 3.10 and 3.11 the appearance of the terms σ_{xx}, σ_{xy} and σ_{yy}. These terms are crucial when investigating the formulation to use. It has been assumed in the past that the unrestricted formulation is superior to the restricted. This assumption is based on the observation that continuity is not actually satisfied, in a numerical sense, and therefore using it to reduce the equations is inappropriate. Although this may be true, in the limit as the order of any finite element approximation is increased the error in the continuity equation, as well as the momentum equations, are reduced. In either case, unless a sufficient number and order of the elements is used the numerical solution is not the exact solution anyway. We will investigate these cases and show the choice of the formulation is based on the problem at hand.

The reduced Stokes equations are shown in equations . These equations differ not only in their partial differential equation but also in their boundary condition.

Draft

9"

Copyright Dr. R. Fithen

6"

Weighted Residual Formulation of Reduced Stokes Equations

Continuity:

$$\int_x \int_y w_p \left[\frac{\partial u}{\partial x} + \frac{\partial v}{\partial y} \right] dydx = 0 \tag{3.12}$$

X-Momentum:

$$\begin{aligned} \int_x \int_y \left[w_u \rho \frac{\partial u}{\partial t} - \rho w_u g_x + \mu \left(\frac{\partial w_u}{\partial x} \frac{\partial u}{\partial x} + \frac{\partial w_u}{\partial y} \frac{\partial u}{\partial y} \right) + w_u \frac{\partial p}{\partial x} \right] dydx \\ = \oint w_u \left[\mu \left(\frac{\partial u}{\partial x} n_x + \frac{\partial u}{\partial y} n_y \right) \right] d\mathcal{S} \end{aligned} \tag{3.13}$$

Y-Momentum:

$$\begin{aligned} \int_x \int_y \left[w_v \rho \frac{\partial v}{\partial t} - \rho w_v g_y + \mu \left(\frac{\partial w_v}{\partial x} \frac{\partial v}{\partial x} + \frac{\partial w_v}{\partial y} \frac{\partial v}{\partial y} \right) + w_v \frac{\partial p}{\partial y} \right] dydx \\ = \oint w_v \left[\mu \left(\frac{\partial v}{\partial x} n_x + \frac{\partial v}{\partial y} n_y \right) \right] d\mathcal{S} \end{aligned} \tag{3.14}$$

Draft

9"

Copyright Dr. R. Fithen

6"
9"
Draft

Chapter 4

Penalty Formulation

Penalty formulation were developed ... We first develop the penalty formulation for Stokes equations followed by a formulation of Navier-Stokes equations.

In two dimensions the constrained Stokes equations are,

$$\rho\frac{\partial u}{\partial t} = f_x - \frac{\partial p}{\partial x} + \mu\left(\frac{\partial^2 u}{\partial x^2} + \frac{\partial^2 u}{\partial y^2}\right) \tag{4.1}$$

$$\rho\frac{\partial v}{\partial t} = f_y - \frac{\partial p}{\partial y} + \mu\left(\frac{\partial^2 v}{\partial x^2} + \frac{\partial^2 v}{\partial y^2}\right) \tag{4.2}$$

$$\frac{\partial u}{\partial x} + \frac{\partial v}{\partial y} = 0 \tag{4.3}$$

Subject to the natural boundary conditions:

$$b_x = \mu\frac{\partial u}{\partial x}n_x + \mu\frac{\partial u}{\partial y}n_y - pn_x \tag{4.4}$$

$$b_y = \mu\frac{\partial v}{\partial x}n_x + \mu\frac{\partial v}{\partial y}n_y - pn_y \tag{4.5}$$

and to the essential boundary conditions,

$$u\left(x, y, t\right) = u_s \tag{4.6}$$

$$v\left(x, y, t\right) = v_s \tag{4.7}$$

as well as the initial conditions,

$$u\left(x, y, 0\right) = u_{ic} \tag{4.8}$$

$$v\left(x, y, 0\right) = v_{ic} \tag{4.9}$$

The unconstrained Stokes equations may be written as

$$\rho\frac{\partial u}{\partial t} = f_x - \frac{\partial p}{\partial x} + \frac{\partial}{\partial x}\left(2\mu\frac{\partial u}{\partial x}\right) + \frac{\partial}{\partial y}\left[\mu\left(\frac{\partial u}{\partial y} + \frac{\partial v}{\partial x}\right)\right] \tag{4.10}$$

Copyright Dr. R. Fithen

$$\rho\frac{\partial v}{\partial t} = f_y - \frac{\partial p}{\partial y} + \frac{\partial}{\partial y}\left(2\mu\frac{\partial v}{\partial y}\right) + \frac{\partial}{\partial x}\left[\mu\left(\frac{\partial u}{\partial y} + \frac{\partial v}{\partial x}\right)\right] \tag{4.11}$$

$$\frac{\partial u}{\partial x} + \frac{\partial v}{\partial y} = 0 \tag{4.12}$$

Subject to the natural (stress based) boundary conditions:

$$t_x = \tau_{xx}n_x + \tau_{xy}n_y = 2\mu\frac{\partial u}{\partial x}n_x + \mu\left(\frac{\partial u}{\partial y} + \frac{\partial v}{\partial x}\right)n_y - pn_x \tag{4.13}$$

$$t_y = \tau_{yy}n_y + \tau_{xy}n_x = 2\mu\frac{\partial v}{\partial y}n_y + \mu\left(\frac{\partial u}{\partial y} + \frac{\partial v}{\partial x}\right)n_x - pn_y \tag{4.14}$$

and to the essential boundary conditions,

$$u\left(x,y,t\right) = u_s \tag{4.15}$$

$$v\left(x,y,t\right) = v_s \tag{4.16}$$

as well as the initial conditions,

$$u\left(x,y,0\right) = u_{ic} \tag{4.17}$$

$$v\left(x,y,0\right) = v_{ic} \tag{4.18}$$

Say something about free-surface verses internal developed flows and the boundary conditions and use of higher order elements for accuracy etc.

The formulation for the mixed method may be obtained as shown below...

$$\begin{aligned}
0 &= \int_x\int_y \delta u\left[\rho\frac{\partial u}{\partial t} - f_x + \frac{\partial p}{\partial x} - \mu\left(\frac{\partial^2 u}{\partial x^2} + \frac{\partial^2 u}{\partial y^2}\right)\right]dxdy \\
0 &= \int_x\int_y \delta v\left[\rho\frac{\partial v}{\partial t} - f_y + \frac{\partial p}{\partial y} - \mu\left(\frac{\partial^2 v}{\partial x^2} + \frac{\partial^2 v}{\partial y^2}\right)\right]dxdy \\
0 &= \int_x\int_y \delta p\left[\frac{\partial u}{\partial x} + \frac{\partial v}{\partial y}\right]dxdy
\end{aligned} \tag{4.19}$$

Integrating by parts yields...

$$\begin{aligned}
0 &= \int_x\int_y \left[\delta u\left(\rho\frac{\partial u}{\partial t} - f_x\right) - \frac{\partial \delta u}{\partial x}p + \mu\left(\frac{\partial \delta u}{\partial x}\frac{\partial u}{\partial x} + \frac{\partial \delta u}{\partial y}\frac{\partial u}{\partial y}\right)\right]dxdy \\
&\quad - \oint \delta u\left\{\mu\frac{\partial u}{\partial x}n_x + \mu\frac{\partial u}{\partial y}n_y - pn_x\right\}dS \\
0 &= \int_x\int_y \left[\delta v\left(\rho\frac{\partial v}{\partial t} - f_y\right) - \frac{\partial \delta v}{\partial y}p + \mu\left(\frac{\partial \delta v}{\partial x}\frac{\partial v}{\partial x} + \frac{\partial \delta v}{\partial y}\frac{\partial v}{\partial y}\right)\right]dxdy \\
&\quad - \oint \delta u\left\{\mu\frac{\partial v}{\partial x}n_x + \mu\frac{\partial v}{\partial y}n_y - pn_y\right\}dS \\
0 &= \int_x\int_y \delta p\left[\frac{\partial u}{\partial x} + \frac{\partial v}{\partial y}\right]dxdy
\end{aligned} \tag{4.20}$$

Draft
Copyright Dr. R. Fithen

If shape functions are.....may not have to be unequal....

$$u = \sum_{j=1}^{n} \psi_j^e u_j \tag{4.21}$$

$$v = \sum_{j=1}^{n} \psi_j^e v_j \tag{4.22}$$

$$p = \sum_{j=1}^{m} \phi_j^e p_j \tag{4.23}$$

$$\delta u = \psi_j^e \tag{4.24}$$

$$\delta v = \psi_j^e \tag{4.25}$$

$$\delta p = \phi_j^e \tag{4.26}$$

Will give a matrix like.....

$$\begin{bmatrix} [M] & [0] & [0] \\ [0] & [M] & [0] \\ [0] & [0] & [0] \end{bmatrix} \begin{pmatrix} (\dot{u}) \\ (\dot{v}) \\ (\dot{p}) \end{pmatrix} + \begin{bmatrix} [G^{11}] & [G^{12}] & [G^{13}] \\ [G^{21}] & [G^{22}] & [G^{23}] \\ [G^{31}] & [G^{32}] & [G^{33}] \end{bmatrix} \begin{pmatrix} (u) \\ (v) \\ (p) \end{pmatrix} = \begin{pmatrix} (F^u) \\ (F^v) \\ (0) \end{pmatrix} \tag{4.27}$$

Where

$$M_{ij} = \int_x \int_y \rho \psi_i \psi_j dx dy \tag{4.28}$$

$$G_{ij}^{11} = G_{ij}^{22} = \int_x \int_y \mu \left(\frac{\partial \psi_i}{\partial x} \frac{\partial \psi_j}{\partial x} + \frac{\partial \psi_i}{\partial y} \frac{\partial \psi_j}{\partial y} \right) dx dy \tag{4.29}$$

$$G_{ij}^{12} = 0 \tag{4.30}$$

$$G_{ij}^{21} = 0 \tag{4.31}$$

$$G_{ij}^{13} = -\int_x \int_y \frac{\partial \psi_i}{\partial x} \phi_j dx dy \tag{4.32}$$

$$G_{ij}^{23} = -\int_x \int_y \frac{\partial \psi_i}{\partial y} \phi_j dx dy \tag{4.33}$$

$$G_{ij}^{13} = G_{ji}^{31} \tag{4.34}$$

$$G_{ij}^{23} = G_{ji}^{32} \tag{4.35}$$

$$G_{ij}^{33} = 0 \tag{4.36}$$

$$F_i^u = \int_x \int_y f_x \psi_i dx dy + \oint \psi_i \left\{ \left(\mu \frac{\partial u}{\partial x} - p \right) n_x + \mu \frac{\partial u}{\partial y} n_y \right\} dS \tag{4.37}$$

$$F_i^v = \int_x \int_y f_y \psi_i dx dy + \oint \psi_i \left\{ \mu \frac{\partial v}{\partial x} n_x + \left(\mu \frac{\partial v}{\partial y} - p \right) n_y \right\} dS \tag{4.38}$$

6"
9"
Draft
Copyright Dr. R. Fithen

6"

If we rewrote our matrix system 4.27 to look like,

$$\begin{aligned} [\mathcal{M}^e]\,(\dot{\mathcal{U}}) + [\mathcal{K}^e]\,(\mathcal{U}) - [\mathcal{C}^e]\,(\mathcal{P}) &= (\mathcal{F}^e) \\ [\mathcal{C}^e]^T\,(\mathcal{U}) + \frac{1}{\epsilon}\left[M_g^e\right](\mathcal{P}) &= 0 \end{aligned} \tag{4.39}$$

Where

$$[\mathcal{M}^e] = \begin{bmatrix} [M] & [0] \\ [0] & [M] \end{bmatrix} \tag{4.40}$$

$$[\mathcal{K}^e] = \begin{bmatrix} \begin{bmatrix} G^{11} \\ G^{21} \end{bmatrix} & \begin{bmatrix} G^{12} \\ G^{22} \end{bmatrix} \end{bmatrix} \tag{4.41}$$

$$[\mathcal{C}^e] = -\begin{bmatrix} \begin{bmatrix} G^{13} \\ G^{23} \end{bmatrix} \end{bmatrix} \tag{4.42}$$

$$\left[M_g^e\right] = \int_x \int_y \phi_i \phi_j dx dy \tag{4.43}$$

and ϵ is a very very large arbitrary number, the penalty parameter. Rearrange equation 4.39 we get an equation devoid of the pressure term.

$$(\mathcal{P}) = -\epsilon\left[M_g^e\right][\mathcal{C}^e]^T\,(\mathcal{U}) \tag{4.44}$$

or

$$[\mathcal{M}^e]\,(\dot{\mathcal{U}}) + [\mathcal{K}^e]\,(\mathcal{U}) + \epsilon\,[\mathcal{C}^e]\left[M_g^e\right][\mathcal{C}^e]^T\,(\mathcal{U}) = (\mathcal{F}^e) \tag{4.45}$$

From this equation the penalty term may easily seen as

$$\left[\mathcal{K}^{Pen}\right] = [\mathcal{C}^e]\left[M_g^e\right][\mathcal{C}^e]^T \tag{4.46}$$

Draft
9"
Copyright Dr. R. Fithen

6"

Bibliography

[1] M. Abramowitz and I. A. Stegun, *Handbook of mathematical functions with formulas, graphs, and mathematical tables*, Dover, 1972.

[2] Vedat S. Arpaci, *Convection heat transfer*, Prentice Hall, 1984.

[3] Canuto, Hussaini, Quarteroni, and Zang, *Spectral methods in fluid dynamics*, Springer Verlag, 1988.

[4] E. Erturk, T.C. Corke, and C. Gokcol, *Numerical solutions of 2-d steady incompressible driven cavity flow at high reynolds numbers*, International Journal for Numerical Methods in Fluids **48** (2005), 747–774.

[5] L.S.G. Kovasznay, *Laminar flow behind a two-dimensional grid*, Proc. Camb. Phil. Soc. 44 (1948).

[6] J. L. Kueny and G. Binder, *Viscous flow over backward facing steps - an experimental investigation*, Analysis of laminar flow over a backward facing step (Morgan, Periaux, and Thomasset, eds.), Vieweg & Sons, 1984.

[7] Leonard Meirovitch, *Computational methods in structural dynamics*, Springer, 1980.

[8] Bruce R. Munson, Donald F. Young, and Theodore H. Okiishi, *Fundamentals of fluid mechanics*, John Wiley & Sons.

[9] A. Nadai, *Theory of flow and fracture of solids*, John Wiley & Sons, 1963.

[10] Ronald L. Panton, *Incompressible flow*, John Wiley & Sons, 2005.

[11] A. G. Peano, *Hierarchies of conforming finite elements for plane elasticity and plate bending*, Comp. & Maths. with Appl. **2** (1976), 211–224.

[12] _____, *Conforming approximations for kirchhoff plates and shells*, Int. J. Num. Meth. Engng. **14** (1979), 1273–1291.

[13] J. N. Reddy, *An introduction to the finite element method*, John Wiley & Sons, 2005.

[14] Barna Szabo and Ivo Babuska, *Finite element analysis*, Wiley-Interscience, 1991.

[15] G. H. Wannier, *A contribution to the hydrodynamics of lubrication*, Quarterly of Applied Mathematics **8** (1950), 1–32.

Draft

9"

Copyright Dr. R. Fithen

6"

[16] Frank M. White, *Viscous fluid flow*, McGraw-Hill, 2005.

[17] O. C. Zienkiewicz, R. L. Taylor, and J.Z. Zhu, *The finite element method*, Butterworth-Heinemann, 2005.

Draft

9"

Copyright Dr. R. Fithen